Chapter 4

Major ions, Sr, Ba and $^{87}Sr/^{86}Sr$ in the Yamuna River System: Chemical weathering and CO_2 consumption in the Himalaya

4.1 INTRODUCTION

Chemical and isotopic investigation of rivers provide useful and important information on the source(s) of major ions, trace elements and isotopes to them, elemental and isotopic fluxes to the sea, chemical weathering rates in the catchment they drain and CO_2 drawdown in their basins. Knowledge on these aspects is essential in assessing the importance of chemical weathering of silicates as a negative feedback in stabilizing the global temperature on a multi-million year time scale (Berner and Berner, 1997). Further, characterization of sources of Sr and its isotopes in rivers draining the Himalaya have implications to interpretation of marine Sr isotope records.

The rivers draining the Himalaya assume global importance as they contribute significantly to the global budget of water and sediment discharge. Draining a young and active mountain chain, they regulate marine geochemistry of a number of elements and isotopes. In recent years, these rivers, especially those draining the southern slopes of the Himalaya, have caught attention of several workers because of possible connection between the uplift of the Himalaya and the Cenozoic climate change (Raymo and Ruddiman, 1992). In the "tectonics-weathering-climate" hypothesis, uplift of the Himalaya has been invoked as a possible driver for the Cenozoic cooling, through uplift induced intense silicate weathering and consequent enhanced CO_2 drawdown from the atmosphere. This hypothesis stems from observation that $^{87}Sr/^{86}Sr$ of seawater started rising steadily since the initiation of the uplift of the Himalaya and the idea that $^{87}Sr/^{86}Sr$ in rivers can be used as a proxy of silicate weathering. Testing such a hypothesis requires estimation of silicate weathering rates and CO_2 drawdown in the region and proper characterization of sources of Sr in these river systems in the Himalaya. If, for example, the $^{87}Sr/^{86}Sr$ in these rivers are regulated by lithologies other than silicates, then the above hypothesis would not stand valid.

Previous work on rivers draining the southern slopes of the Himalaya include those of Sarin et al. (1989, 1992a), Pande et al. (1994) and Krishnaswami et al. (1999) on the major ion chemistry of the headwaters of the Ganga, Indus and the Ghaghara. These studies brought out the dominance of carbonate weathering in contributing to the dissolved load of these rivers and provided estimates of CO_2 consumption rates via silicate weathering in their drainage basins. Galy and France-Lanord (1999), based on studies of major ions and $\delta^{13}C$ of dissolved inorganic carbon in the Kali Gandaki basin, assessed the role of carbonic and

sulphuric acids in contributing protons to the weathering reactions and derived the alkalinity fluxes and CO_2 consumption rates. More recently, Karim and Veizer (2000) carried out extensive studies on the headwaters of the Indus to determine the sources of cations to these rivers. On a global scale, Gaillardet et al. (1999), based on a compilation of data on major rivers, estimated the contemporary CO_2 consumption fluxes via silicate weathering in the drainage basins of the rivers draining the Himalaya. Handa (1972) and Jha et al. (1988) have also reported major ion composition of the Yamuna river. These measurements, however, are mainly in the lower reaches of the Yamuna and its tributaries in the plains.

The contribution of Sr from the rivers draining the Himalayan region and their $^{87}Sr/^{86}Sr$ has much significance in the mass balance of marine Sr and its isotopic composition (Richter et al., 1992). The issue of sources of Sr to these rivers, however, has been a matter of controversy among various workers. Studies on Sr isotopes in Himalayan river systems showed that the rivers draining the Himalaya, particularly its southern slopes, have both high Sr concentration and $^{87}Sr/^{86}Sr$ compared to other major rivers of the world (Krishnaswami et al., 1992; Palmer and Edmond, 1989, 1992; Trivedi et al., 1995). Available information on the sources of Sr isotopes, mass balance of Sr and $^{87}Sr/^{86}Sr$ in the river systems in the Himalaya have been diverse and at times controversial. Krishnaswami et al. (1992) and Edmond (1992) suggested silicates as the important source of high $^{87}Sr/^{86}Sr$, whereas Palmer and Edmond (1992) proposed metamorphosed carbonates to be responsible for the high radiogenic composition in these rivers. Singh et al. (1998) and Krishnaswami et al. (1999), based on studies of Precambrian carbonate outcrops in the Lesser Himalaya, concluded that on a basin wide scale silicate weathering exerts dominant control on high $^{87}Sr/^{86}Sr$ of many of the Ganga-Ghaghara-Indus source waters though carbonates might be important in particular streams. Their data synthesis also brought out the need for additional source(s) other than silicates and carbonates occurring in the catchment to balance the Sr budget of these rivers. Galy et al. (1999) concluded that silicates in the Lesser Himalaya and in the Siwaliks are sources of the high $^{87}Sr/^{86}Sr$ in the Ganga-Brahmaputra rivers. Quade et al. (1997) based on a study of soil and detrital carbonates in river basins in Nepal proposed that carbonates exert dominant control on high $^{87}Sr/^{86}Sr$ in the rivers in the Himalaya. Blum et al. (1998) and Harris et al. (1998), based on major ion chemistry and Sr isotopes in the Bhote Kosi and Raikhot rivers, underlined the importance of weathering of carbonates and

disseminated calcites in influencing the Sr budget and its radiogenic composition in the rivers draining the Himalaya.

This chapter presents and discusses major ion composition, Sr, Ba and $^{87}Sr/^{86}Sr$ in headwaters of the Yamuna River System in the Himalaya. The data have been used to assess the relative contributions of various lithologies to major ions of these rivers, to derive CO_2 consumption rates in the basin via silicate weathering and to estimate apparent activation energy for overall silicate weathering in the basin. Attempts are also made to establish a balance for dissolved Sr in the YRS and to assess relative control of various lithologies in regulating the Sr isotopic composition of these rivers. Some of the controversial issues such as the role of vein calcites in influencing the Sr isotopic compositions of rivers have also been addressed in relation to the Yamuna system. The results of CO_2 drawdown in the YRS basin has been compared with those of the headwaters of the Ganga-Ghaghara-Indus to obtain an estimate of contemporary CO_2 drawdown in the southern slopes of the Himalaya and its significance on a global context.

4.2 RESULTS AND DISCUSSION

4.2.1 Major ion chemistry

The data on major ions, silica and TDS in the rivers and springs are given in Table 4.1. These include samples from the YRS, the Ganga at Rishikesh (at the foothills of the Himalaya) and the Bandal, a stream flowing through the phosphorite-blackshale-carbonate formations near Maldeota. The spring samples analyzed are from the Kempti Fall (RW98-7, RW99-9) and Shahashradhara (RW99-60). The chemical composition of the bed sediments from rivers/streams of the YRS and granites collected around Hanuman Chatti are given in Table 4.2. The temperatures of the water samples were measured only during summer (June 1999) and monsoon (September 1999) expeditions. It ranged from 10-30 °C, the lower temperatures are typical of samples from the upper reaches (Appendix-2.1). The river waters are mildly alkaline in nature, covering a pH range of 7.7-9.2, with bulk of the samples having values in a narrow range of 8.5±0.2 (Appendix-2.1).

Table 4.1 Major ions, Sr, Ba and $^{87}Sr/^{86}Sr$ in the Yamuna River System, the Ganga and Spring waters.

Code[a]	Season[b]	Na µM	K µM	Ca µM	Mg µM	F µM	Cl µM	NO_3 µM	SO_4 µM	Alk. µM	Si µM	TDS mg ℓ^{-1}	Sr nM	Ba nM	$^{87}Sr/^{86}Sr$
Yamuna main stream															
RW98-16	PM	67	56	388	100	16	30	13.5	113	780	92	88	381	64	0.75158
RW99-13	S	81	45	397	89	18	43	b.d.	129	834	77	91	287	47	0.75543
RW98-20	PM	89	55	392	104	15	36	14.6	100	855	112	93	412	77	0.75725
RW98-25	PM	110	52	406	133	11	52	13.0	76	960	126	100	422	70	0.74985
RW99-19	S	185	46	450	122	n.m.	106	b.d.	116	1022	100	110	374	47	
RW99-17	S	133	47	438	97	n.m.	54	b.d.	126	944	91	102	314	49	
RW98-22	PM	117	52	422	133	10	53	13.3	76	990	127	103	468	77	0.74887
RW99-18	S	171	47	511	155	n.m.	97	b.d.	117	1215	100	125	343	53	
RW98-15	PM	108	50	500	186	10	50	12.5	72	1260	140	124	386	77	0.74598
RW98-14	PM	110	48	525	211	9.2	50	12.1	63	1445	144	136	402	81	0.74495
RW99-11	S	168	42	576	204	n.m.	84	b.d.	108	1480	114	144	486	69	
RW98-12	PM	136	35	504	167	6.5	46	19.0	66	1260	176	125	903	85	0.73757
RW98-9	PM	123	40	611	308	7.6	42	17.9	220	1440	158	157	1164	145	0.72595
RW99-51	M	60	50	332	76	6.7	23	6.6	40	894	109	85	309	37	0.73964
RW98-6	PM	136	39	664	299	7.7	41	18.2	216	1575	169	168	1347	159	0.72831
RW99-30	S	206	48	835	354	n.m.	96	7.5	417	1725	115	205	1494	138	
RW99-64	M	119	39	590	186	7.1	34	12.4	154	1344	155	140	993	84	0.73317
RW99-31	S	175	44	720	310	12	75	b.d.	405	1357	96	172	1461	134	0.72556
RW99-53	M	76	51	352	100	7.8	24	20.6	93	1041	112	102	646	63	0.73263
RW98-1	PM	112	46	481	171	8.0	29	28.4	101	1085	167	117	728	131	0.73518
RW99-2	S	221	46	706	272	n.m.	56	46	165	1943	221	194	921	180	
RW99-58	M	92	42	452	130	6.2	24	24.5	100	1039	137	109	522	76	0.73446
RW98-4	PM	255	52	1019	497	8.1	60	35	333	2369	211	254	1802	310	0.72356
RW99-5	S	306	49	967	661	n.m.	73	5.7	556	2508	193	285	2044	269	
RW99-55	M	262	61	920	344	9.8	67	44	288	2900	183	274	1484	349	0.72447
RW98-33	PM	213	61	928	451	10	58	33.5	268	2250	220	236	1513	315	0.72657

RW99-7	S	242	85	948	448	11	56	5.8	321	2608	204	262	1664	321	0.72657
RW99-54	M	122	58	500	173	9.5	32	15.7	192	1520	146	151	895	158	0.72624
Tributaries															
RW98-17	PM	38	68	182	41	3.2	7.7	26.9	27	473	98	51	197	77	0.77113
RW98-18	PM	33	32	91	24	2.2	5.7	15.8	11	293	87	32	126	25	0.79320
RW99-14	S	42	31	107	21	n.m.	9.8	b.d.	28	347	83	36	121	17	
RW98-19	PM	41	44	413	113	3.1	10.3	14.9	61	945	117	94	352	77	0.73992
RW99-16	S	49	46	617	155	n.m.	18.4	b.d.	137	1373	106	135	326	82	
RW99-15	S	50	31	174	28	n.m.	13.1	23.9	39	450	104	49	139	45	
RW98-13	PM	139	35	796	404	5.0	42	2.0	58	2205	201	200	649	137	0.73754
RW99-12	S	249	49	1075	732	n.m.	73	b.d.	111	3372	238	302	993	155	
RW98-23	PM	172	79	619	232	n.m.	42	b.d.	31	1740	220	161	889	871	
RW98-21	PM	107	33	538	284	4.3	37	4.5	32	1560	163	142	609	102	0.73679
RW99-20	S	172	41	967	545	n.m.	76	b.d.	79	2672	200	243	683	100	
RW98-24	PM	156	20	535	312	4.1	36	16.0	26	1650	232	153	689	38	0.73748
RW98-26	PM	89	49	133	53	6.9	12.2	8.3	19	450	200	53	259	39	0.77495
RW99-21	S	184	66	254	84	12	32	b.d.	44	843	253	91	379	50	0.76858
RW99-27	S	88	47	247	47	n.m.	26	10.5	102	533	110	65	324	62	
RW98-27	PM	64	45	182	35	11	19	14.4	62	383	116	49	200	47	0.76059
RW99-22	S	58	36	177	23	n.m.	22	b.d.	82	389	77	47	156	29	
RW98-28	PM	73	45	189	40	11	26	13.2	58	383	119	50	221	46	0.76145
RW99-26	S	58	35	148	22	n.m.	24	b.d.	72	317	67	40	168	29	
RW98-29	PM	78	46	221	50	10	23	15.0	62	495	138	60	256	57	0.74954
RW99-28	S	66	38	199	30	n.m.	25	b.d.	81	378	79	48	225	36	
RW98-31	PM	125	23	727	254	4.8	35	26	159	1575	206	166	1071	191	0.72927
RW99-23	S	152	28	998	470	n.m.	43	4.2	257	2377	176	238	1037	228	
RW99-25	S	82	44	251	52	n.m.	30	b.d.	99	550	92	65	274	44	
RW98-30	PM	98	37	436	160	8.3	31	17.9	100	990	163	107	594	119	0.73676
RW99-24	S	137	32	833	378	n.m.	41	5.0	217	1980	157	200	835	172	
RW98-5	PM	204	20	750	209	4.7	36	32	127	1820	239	181	1941	87	0.73684

RW99-62	M	217	19	772	214	4.6	33	26	150	1836	222	184	1438	68	0.73972
RW98-32	PM	152	52	808	411	11	29	20.6	581	1395	186	202	2196	177	0.72693
RW99-29	S	155	50	822	392	10	31	3.4	777	1097	105	197	2199	123	0.72292
RW99-63	M	108	42	621	243	8.5	22	18.9.	340	1113	138	146	1343	99	0.72835
RW98-8	PM	154	28	1099	957	9.7	39	28	1052	2115	217	318	4429	391	0.71502
RW99-10	S	227	30	2358	2116	n.m.	52	b.d.	3072	2640	196	622	13410	282	
RW99-52	M	162	28	1172	842	9.7	41	6.5	1139	2146	228	328	4772	296	0.71473
RW98-2	PM	259	50	1658	1065	9.8	48	58	1115	2834	231	399	4546	439	0.71920
RW99-3	S	298	53	1807	1621	8.3	51	22	2046	3524	186	547	4638	446	0.72050
RW99-57	M	258	44	1404	736	8.5	42	38	880	2697	217	348	3517	338	0.71954
RW98-3	PM	275	42	954	460	6.7	77	39	395	1867	241	229	1679	n.m.	0.72107
RW99-4	S	372	49	1064	776	n.m.	54	b.d.	923	2233	167	309	2915	231	
RW99-56	M	306	47	1084	424	6.8	94	54	386	2524	230	274	1809	274	0.72060
RW98-10	PM	204	33	1512	959	13	57	25	1226	2610	227	384	5758	538	0.71415
RW99-65	M	187	30	1429	623	10	30	b.d.	707	2614	234	320	4280	347	0.71591
RW98-11	PM	330	46	1893	1080	11	225	164	975	3840	351	479	2491	764	0.71491
RW99-1	S	349	33	1491	1213	n.m.	256	151	714	4257	378	468	1793	725	
RW99-61	M	324	55	1887	972	11	225	119	822	3920	303	461	2870	530	0.71421
Ganga and Bandal															
RW98-34	PM	102	45	452	195	11	27	18.2	165	1035	151	117	626	n.m.	0.73856
RW99-6	S	106	46	446	176	11	24	17.5	204	1014	81	115	712	78	0.73657
RW99-59	M	76	37	397	150	8.6	21	10.6	145	891	116	99	507	72	0.73849
RW99-8	S	116	45	1226	1260	7.1	35	9.0	909	3020	141	366	2108	257	0.72116
Springs															
RW98-7	PM	54	27	2520	2035	n.m.	49	19.0	2913	2340	142	587	12794	n.m.	0.70954
RW99-9	S	74	23	3805	3187	n.m.	34	12.8	5454	3406	145	975	25200	239	
RW99-60	M	281	53	13366	3942	n.m.	3.4	b.d.	15401	4623	175	2412	62086	83	0.70972

[a]RW - river water, [b]S = summer, M = monsoon, PM = post-monsoon. n.m.: not measured, b.d.; below detection limit

Table 4.2 Chemical composition of bed sediments and granites from the YRS basin.

Sample Code[a)]	Na (%)	K (%)	Ca (%)	Mg (%)	Al (%)	Fe (%)	Carb. (%)[b)]	Sr (ppm)	Ba (ppm)
Sediments									
RS98-1	0.98	1.46	1.57	0.82	4.51	2.36	3.27	69	319
RS98-2	0.86	1.99	2.18	1.47	5.90	3.17	7.29	63	471
RS98-3	0.57	1.30	0.80	0.73	4.05	2.15	1.48	51	278
RS98-4	1.04	1.56	1.55	0.93	4.44	0.47	3.43	77	367
RS98-5	1.29	2.49	0.58	0.91	7.11	3.27	1.16	52	447
RS98-5R	1.21	2.51	0.58	0.92	6.94	3.06	n.m.	54	484
RS98-6	1.21	1.43	1.88	1.09	4.10	1.91	3.77	75	297
RS98-8	0.37	1.60	10.1	5.79	3.02	1.37	43.5	156	535
RS98-9	1.06	1.32	1.79	0.98	3.89	1.89	2.96	78	286
RS98-11	0.47	1.92	0.39	0.82	5.24	2.35	0.11	56	497
RS98-12	1.14	1.40	1.45	0.88	3.82	1.61	1.71	74	286
RS98-13	1.09	1.97	2.29	1.97	5.80	2.27	3.93	71	427
RS98-13R	1.03	2.01	2.27	2.01	6.03	2.87	n.m.	74	433
RS98-14	1.19	1.37	1.50	0.78	3.71	1.91	1.44	62	245
RS98-18	1.64	3.01	0.81	0.97	5.86	2.04	0	64	507
RS98-19	0.92	1.14	2.98	1.00	5.05	3.65	5.48	85	265
RS98-19R	0.93	n.m.	2.99	1.00	4.89	3.51	n.m.	88	272
RS98-20	1.54	2.01	1.74	0.76	4.86	1.92	2.23	91	400
RS98-21	0.69	1.51	0.48	0.53	3.15	1.24	0.40	48	319
RS98-22	1.31	1.52	1.50	0.83	4.30	2.11	1.63	72	285
RS98-22R	1.29	1.55	1.48	0.84	4.32	1.89	n.m.	72	296
RS98-25	1.38	1.77	1.39	0.88	4.53	2.02	1.16	75	328
RS98-26	0.63	1.04	0.73	0.52	3.28	2.81	0	45	201
RS98-27	1.31	1.76	0.92	0.59	4.89	2.12	0	98	422
RS98-28	1.26	1.64	0.88	0.54	4.47	1.98	0	94	394
RS98-29	1.05	1.26	0.84	0.43	4.29	3.00	0	75	303
RS98-30	0.94	1.65	1.56	0.86	5.23	4.24	3.53	74	420
RS98-31	0.88	2.24	2.06	1.14	6.49	3.37	6.47	65	549
RS98-32	1.19	1.47	1.44	0.79	4.97	2.63	2.56	104	381
RS98-33	0.98	1.59	1.29	0.91	5.22	2.92	2.84	78	419
Granites									
GR98-1	3.67	1.58	1.13	0.23	n.m.	n.m.	0.71	90	122
GR98-2	4.11	3.80	0.80	0.54	n.m.	n.m.	0.16	130	377
GR99-1	3.51	3.64	1.21	0.50	n.m.	n.m.	0.76	153	396
GR99-2	3.63	3.99	0.71	0.35	n.m.	n.m.	0.92	110	333

[a)]RS: bed sediment, GR: granite, n.m.: not measured, R: replicate analysis. [b)]calculated assuming all carbonates to be $CaCO_3$.

The total cation charge (TZ^+) balances that of the total anions (TZ^-) in most of the samples. Regression analysis of TZ^+ and TZ^- in the YRS yield a line with a slope of 0.98±0.01 (indistinguishable from 1.0 within error) and $r^2 = 0.989$ (Fig. 4.1).

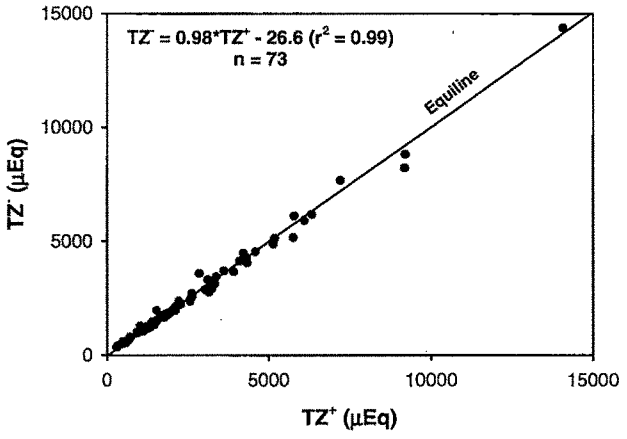

Fig. 4.1 Plot of TZ^+ vs. TZ^- for the YRS rivers. Most of the samples plot on the equiline.

Out of the 80 samples analyzed (Table 4.1), 68 samples exhibit normalized inorganic charge balance [NICB = $(TZ^+-TZ^-)/TZ^+$] less than 10%, indicating that the major ions measured in this study by and large account for the charge balance. Bulk of the remaining 12 samples had $TZ^->TZ^+$, the cause for which is unclear. The data, however, suggest that the contributions from organic acids and ligands to the charge balance in the YRS samples analyzed is not significant as reported for tropical rivers such as the Nyong (Viers et al., 2000) and those draining the Guayana Shield (Edmond et al., 1995).

The total cations (TZ^+) and total dissolved solids (TDS) in the YRS range from ~300 to ~9200 µEq and ~32 to ~620 mg ℓ^{-1} respectively. Both TZ^+ and TDS show spatial and temporal variations. Spatially, the samples collected from the upper reaches have lower TZ^+ and TDS, temporally the summer (June) samples have more TDS than those collected during post-monsoon (October) and monsoon (September) seasons. Previous studies from our group (Sarin et al., 1989; Singh 1999, unpublished results) have reported major ion composition of the Ganga at Rishikeshand the Yamuna at Saharanpur. The earlier data are compared with those measured in this study in Table 4.3. The results for the Ganga at Rishikesh, are remarkably similar for most of the major ions suggesting that over nearly two decades, its

major ion composition during monsoon has remained nearly the same. For the Yamuna, the data of Sarin et al. (1989) are for samples collected in March, during which no sampling was done in the present study. If, however, March data of Sarin et al. (1989) are compared with those of June samples collected in this study, it is seen that the former show lower concentrations of ions (by 30-40 %) than that measured in this work (Table 4.3). These differences could arise due to intra and/or interannual variations in water chemistry.

Table 4.3 Temporal variations in the Ganga and Yamuna major ion chemistry

Component	**Ganga at Rishikesh[a)]**			**Yamuna at Saharanpur[b)]**	
	Sarin et al., 1989	*Singh, 1999*	*This study*	*Sarin et al., 1989*	*This study*
Ca	353	355	397	590	948
Mg	153	122	150	329	448
Na	59	65	76	203	242
K	38	43	37	45	85
HCO_3	894	900	891	1677	2608
SO_4	121	82	145	251	321
Cl	23	23	21	52	56

[a)]sampled during monsoon (September). [b)]Sarin et al. (1989) sampled during March, this work during June.

The TDS in the YRS, as mentioned earlier, range from ~32 to ~620 mg ℓ^{-1}, with more than 80% of the samples having TDS >80 mg ℓ^{-1} (Table 4.1, Fig. 4.2). The lower TDS values (≤50 mg ℓ^{-1}) are in tributaries of the Yamuna and the Tons in their upper reaches where the lithology is predominantly Higher Himalayan Crystallines (Fig. 2.3). The TDS in the

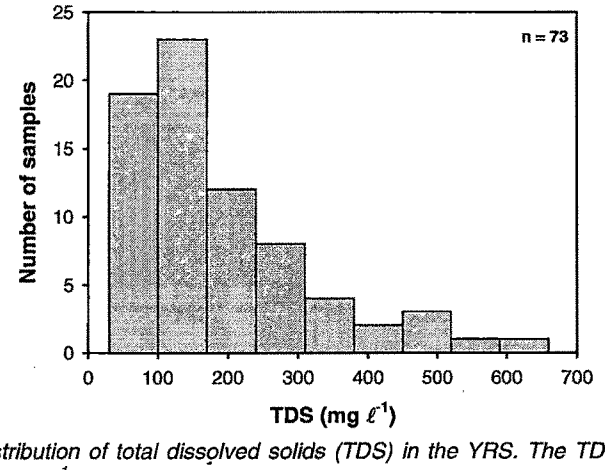

Fig. 4.2 Distribution of total dissolved solids (TDS) in the YRS. The TDS range from ~32 to ~620 mg ℓ^{-1}.

Yamuna even at Hanuman Chatti, however, is quite high, ~90 mg ℓ^{-1}, though the location is only about 10 km downstream of its glacier source. This underlines the significant role of glacier melt waters in contributing to the major ion budget of the Yamuna at this site. Many glacier melt waters from the Himalaya, e.g. Dokriani, Pindari all have high TDS, ~32 to 220 mg ℓ^{-1}, attributed to weathering of carbonates by CO_2 and H_2SO_4 (Hasnain and Thayyen, 1999; Pandey et al., 2001). The relatively high concentration of Ca in the sample at Hanuman Chatti (RW98-16, RW99-13, Table 4.1) supports such a contention. The TDS values of the YRS are higher than those in the headwaters of the Ganga (Sarin et al., 1992) and are either similar to or lower than those in the Indus (Karim and Veizer, 2000; Pande et al. 1994). These TDS values are lower than those in the Kali Gandaki and its tributaries, draining the Tethyan Sedimentary Series (TSS) and Lesser Himalaya (LH), but much higher than those in the Trisuli and its tributaries which drain mainly the Higher Himalayan Crystallines (HHC) in the Nepal Himalaya (Galy and France-Lanord, 1999). The YRS rivers in the lower reaches have TDS similar to those in the Changjiang, Mekong and Xijiang, rivers draining the northern slopes of the Himalaya (Gaillardet et al., 1999).

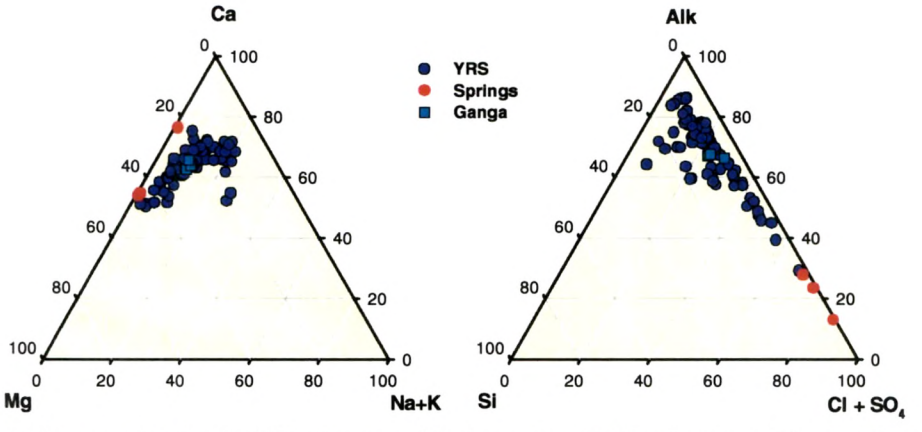

Fig. 4.3 Ternary plots for the YRS, Ganga and Spring waters. Cations for most of the samples plot close to the Ca apex suggestive of dominance of carbonate weathering in the catchment. Anions plot on the mixing line of alkalinity and SO_4+Cl, suggesting contributions from carbonate-evaporite-pyrite weathering (see text).

On a global scale, the TDS in the YRS are generally higher than those in the Amazon, Congo, Niger and in the streams draining the Guayana shield (Boeglin and Probst, 1998; Edmond et al., 1995; Edmond and Huh, 1997; Gaillardet et al., 1997; Negrel et al., 1993) but

are either similar to or lower than those in the rivers draining basaltic terrains such as the Reunion Island and the Deccan Traps (Louvat and Allegre, 1997; Dessert et al., 2001).

Among the cations, Ca is the most abundant followed by Mg, together they constitute ~90% of TZ^+. The major cations decrease as Ca>Mg>Na>K (Table 4.1), a trend similar to that observed in the Ganga headwaters (Sarin et al., 1992). This is clearly evident in the ternary cation plot (Fig. 4.3) in which most of the samples cluster around the Ca apex with a

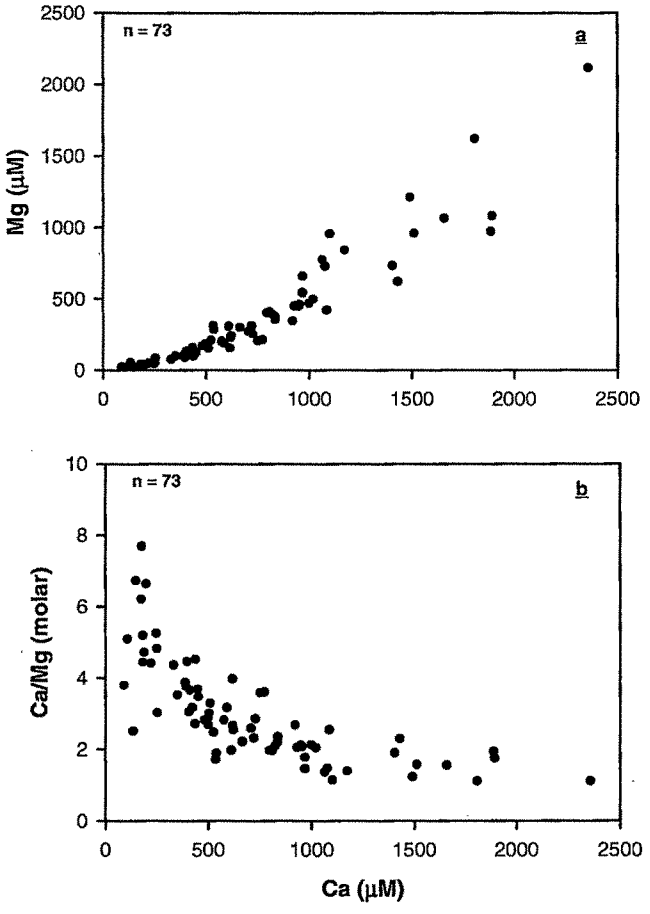

Fig. 4.4 Scatter plot Mg concentration (a) and Ca/Mg molar ratio (b) against Ca in the YRS waters. Mg abundances show a strong positive correlation with Ca suggestive of a common source. Ca/Mg ratios decrease with increasing Ca, dolomite weathering and/or preferential removal of Ca (as calcites) can contribute to the observed trend.

few of them tending towards the Mg apex. This is characteristic of limestone and dolomite weathering, consistent with the lithology of the drainage basin. Mg shows a significant positive correlation with Ca (Fig. 4.4a). The Ca/Mg molar ratios average about 3, with a range from 1.1 to 7.7. The range and mean of Ca/Mg in the YRS are similar to those in the

Ganga headwaters (range: 1.9 to 7.6, mean: 3.3, Sarin et al., 1992a). In the YRS, Ca/Mg decreases with increasing Ca concentration (Fig. 4.4b), low Ca/Mg (1-2) are mainly in streams such as the Aglar, Asan, Giri, Bata and the Yamuna and the *Tons* in the lower reaches (Table 4.1, Fig. 4.4b) all of which flow through terrains abundant in Precambrian

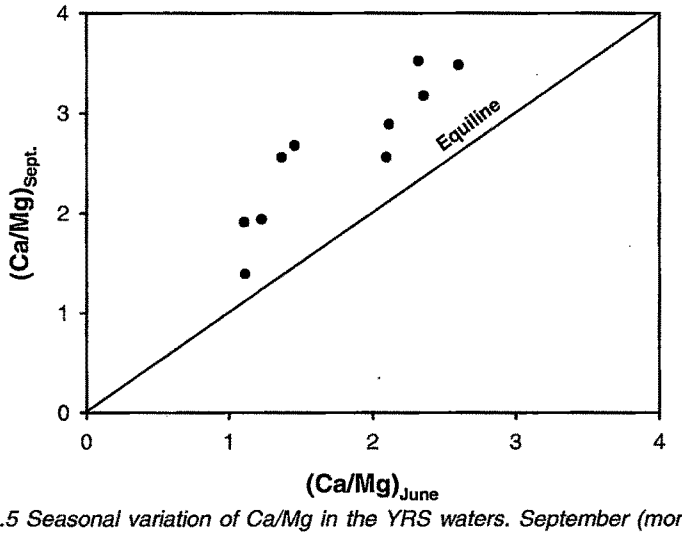

Fig. 4.5 Seasonal variation of Ca/Mg in the YRS waters. September (monsoon) samples have higher Ca/Mg ratios than the June (summer) samples.

carbonates. A likely cause for the low Ca/Mg in these waters is the supply of Ca and Mg via dissolution of dolomites that constitute a major portion of the Precambrian carbonates (Singh et al., 1998). A closer inspection of the data reveals that in samples collected from the lower reaches of the YRS during monsoon have higher Ca/Mg than those collected during the summer season (Fig 4.5). This could be due to relatively rapid dissolution of calcite during the monsoon period when the water flow is high. Alternatively, low Ca/Mg during summer can result if Ca is preferentially removed from the rivers by precipitation (e.g. calcite), a mechanism invoked by Sarin et al. (1989) to explain seasonal variations in Ca/Mg in the Ganga river system in the plains. Calcite precipitation, if any, is more likely to occur during summer than during the monsoon, considering that the cation and alkalinity concentrations are in general higher during summer. To assess whether calcite can precipitate from the waters of the YRS, calcite saturation index (CSI) was calculated using pH, HCO_3 and Ca data following the approach of Drever (1997). These calculations were made for two temperatures, 15 °C and 25 °C, for river waters with temperatures ranging between 10-20 °C

and 20-30 °C respectively. The results show wide range of calcite saturation with bulk of the river waters being supersaturated with calcite (Fig. 4.6).

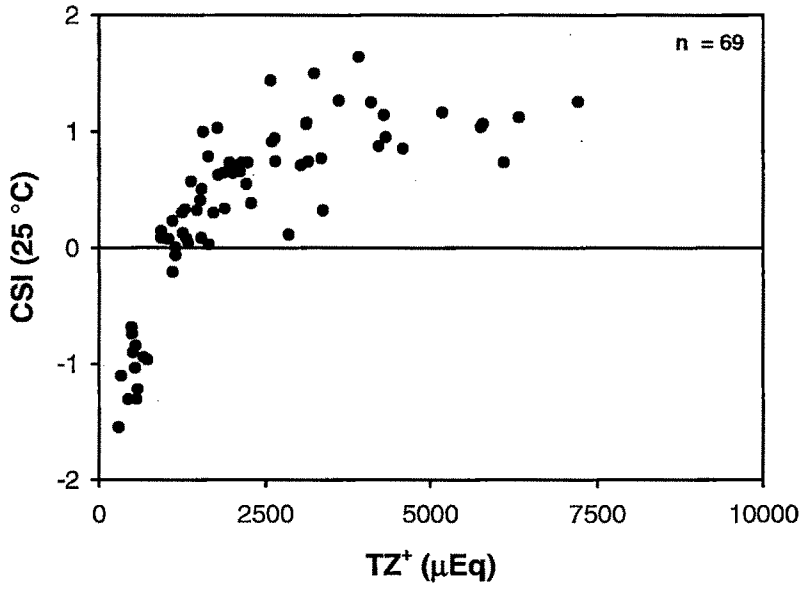

Fig. 4.6 Calcite saturation index (CSI) in the YRS rivers/streams. Bulk of the samples are supersaturated with calcite, the degree of saturation seems to show an increasing trend with total cation charge. Rivers in the upper reaches generally have CSI <0.

The impact of supersaturation on the precipitation of calcite is uncertain, though it is interesting to note that the rivers Aglar, Asan, Giri, Bata, *Tons* at Dehradun, Barni Gad which have low Ca/Mg ratios also have high degree of calcite supersaturation (CSI ≥1). The observation that Ca and Mg concentrations in unacidified river water samples measured several weeks after the collection, is nearly identical to those measured in the acidified samples (Fig. 2.11, Chapter 2), suggests that there is no measurable loss of Ca via precipitation in the laboratory. The lack of nucleation process may be responsible for preventing precipitation of calcite and thereby aid in maintaining its supersaturation. If this result can be extended to YRS rivers, it would indicate that calcite precipitation and preferential loss of Ca may not be a cause for altering Ca/Mg in samples analyzed. This inference, however, needs to be validated through more detailed laboratory and field studies. Use of carbonate content of bed sediments to determine if calcite precipitation occurs, also does not yield unambiguous conclusions. This is because these sediments contain detrital carbonates derived from the drainage basin. Indeed, Galy and France-Lanord (1999), based

on Sr, C and O- isotopic composition of the bed load in rivers of the Nepal Himalaya and Bangladesh and carbonate bedrocks, inferred that the bed carbonates are mainly of detrital origin. Thus, the origin of higher carbonate contents in the bed sediments of the Yamuna and its tributaries draining the lower reaches (Table 4.2) is uncertain, it can either be of detrital origin or of calcite precipitation or both.

The tributaries of the Yamuna and the Tons in their upper reaches, flowing mainly through crystallines, are undersaturated with calcite. These streams are low in TZ^+ and have much less carbonates in their bed sediments. It is seen that in general summer samples have higher CSI values. This is expected as both Ca and alkalinity show higher abundances during summer (Table 4.1). This trend is reflected in the general trend of CSI with TZ^+ (Fig. 4.6).

There is considerable excess of Na over Cl, the range in Na/Cl molar ratio being 1.4 to 7.3 (mean 3.6). This suggests that on an average, contribution of Na from recycled marine salt and evaporite dissolution is only about a third of its abundance and that bulk of Na has to be derived from silicate weathering. Inspite of this, on an average, Na^* and K together [Na^* = (Na-Cl), Na corrected for cyclic salt and evaporite dissolution] constitute only ~10 % of the TZ^+ suggesting that silicate weathering is not a major source of cations to these rivers on a basin wide scale (see later discussion). Godu Gad and Didar Gad, which flow mainly through silicate terrains have Na^*+K contribution to TZ^+ as high as ~25%. These streams also have high SiO_2 contribution to TDS (see discussion below) and highly radiogenic $^{87}Sr/^{86}Sr$ (Table 4.1). K/Na^* molar ratios in the YRS range from 0.1 to 2.2 with an average 0.6. In general, streams in the upper reaches have high K/Na^* (≥ 1). The K/Na^* decreases with increasing Na^* (Fig. 4.7). This decrease is mainly due to increase in Na^* in the lower reaches, the K concentrations in the waters by and large center around 30-50 μM (Table 4.1).

The dissolved silica concentrations of the YRS lie in the range of 67 to 378 μM (Table 4.1). This range is marginally higher than that in the Ganga headwaters (42 to 294 μM; Sarin et al., 1992). The Si concentrations in the YRS rivers are generally similar to those in the rivers draining the Nepal Himalaya (Galy and France-Lanord, 1999) but is lower than those in the rivers draining basaltic rocks (Louvat and Allegre, 1997; Dessert et al., 2001). The dissolved Si concentrations in the rivers draining the northern slopes of the Himalaya, the Changjiang, the Mekong and the Xijiang (Gaillardet et al., 1999) are, in general, lower than those in the YRS rivers. On an average, SiO_2 accounts for ~7 % of the TDS (wt. basis).

Its contribution to the TDS in the YRS streams, varies from ~2 to ~23%, the streams draining predominantly silicates, the Godu Gad and the Didar Gad have higher SiO_2 contribution to TDS whereas the Shahashradhara spring water has the lowest. $(Na^*+K)/(TZ^+)^*$ in the YRS show a significant positive correlation with SiO_2/TDS, the regression line having a slope of 0.68 (r^2 = 0.81, Fig. 4.8). This trend suggests that an increase in relative contribution of silicate (Na*+K) to TZ^+ is accompanied by an increase in silica contribution to the TDS. Further, the trend in Fig. 4.8 is an indication that weathering of silicate minerals is the dominant source of dissolved SiO_2 to the waters and that its supply via quartz dissolution does not seem to play an important role in regulating the dissolved silica budget, an inference attested by low value of the intercept (0.01) of the regression line (Fig. 4.8).

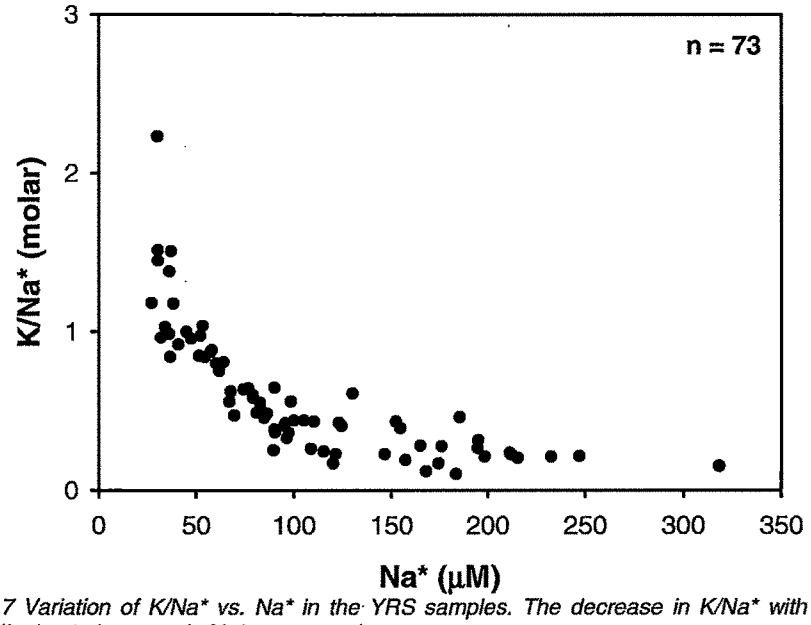

Fig. 4.7 Variation of K/Na vs. Na* in the YRS samples. The decrease in K/Na* with Na* is primarily due to increase in Na* concentration.*

It is also seen from the data (Fig. 4.9) that the Si abundance and TZ^+ are positively correlated, albeit with some scatter especially at higher TZ^+ values. This correlation seems to suggest that the weathering of silicates and other lithologies occur roughly in the same proportion in the drainage basins of the YRS. A possible reason for the scatter at high TZ^+ values could be weathering of carbonates and/or evaporite dissolution, which adds to the TZ^+, but with very little Si. The samples of the Giri (RW99-3) and Aglar (RW99-10), with very high TZ^+ (>7000 μEq), fall far away from the trend set by the other samples. These

rivers drain carbonates of Krol Formations, which have been known to have pockets of gypsum in them. Further, they have high SO_4 (>2000 μM), Ca and Mg, with SO_4>Ca and samples collected from these rivers during post-monsoon have high Re (Chapter 5). It can be

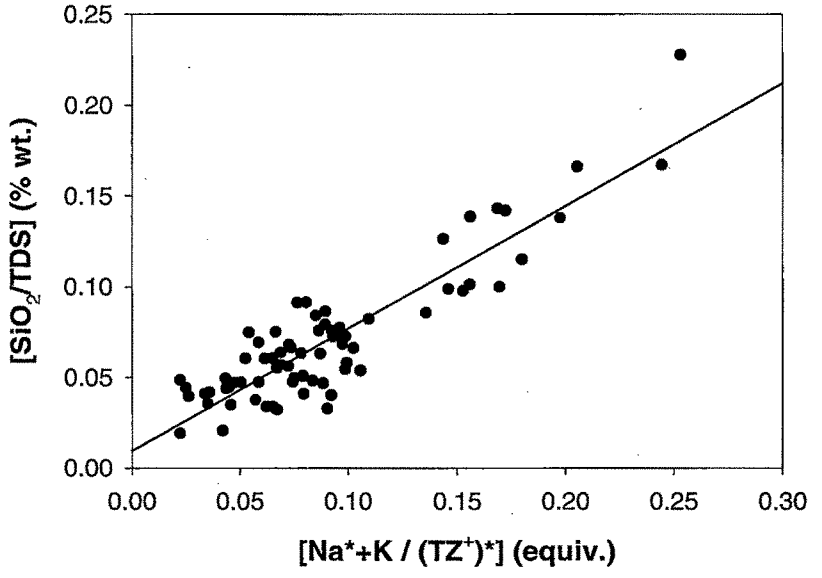

Fig. 4.8 Plot of SiO_2/TDS vs. (Na+K)/TZ^+ for the YRS waters. A strong positive correlation is evident (r^2 = 0.81) indicating that increase in contribution of (Na*+K) to total cations is accompanied by an increase in SiO_2 contribution to TDS. This covariation can be interpreted in terms of supply of SiO_2 and (Na*+K) to rivers via silicate weathering.*

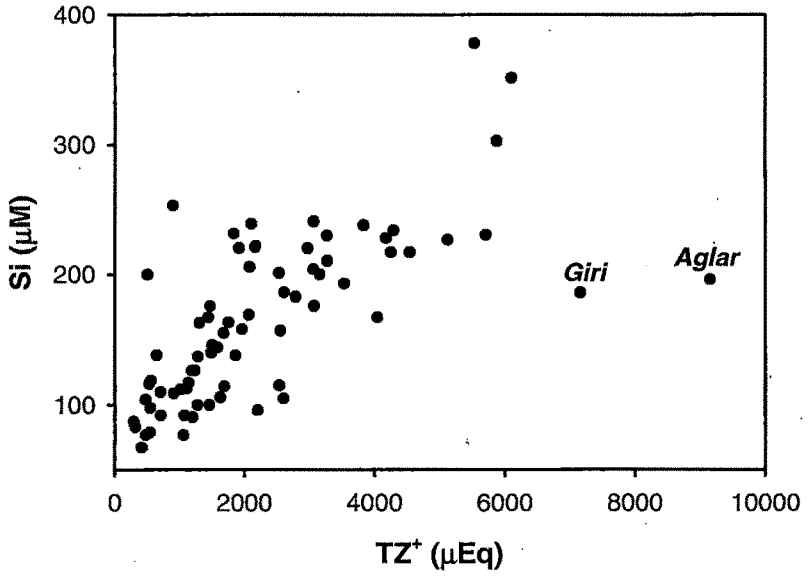

Fig. 4.9 Scatter plot of Si vs. TZ^+ in the YRS waters. A positive correlation is seen with larger scatter at higher TZ^+.

inferred from all these data that the waters in these rivers derive cations mainly from weathering of carbonates by carbonic and sulphuric acids and gypsum dissolution. Consequently they have high TZ^+ and less Si compared to the other rivers.

Carbonate alkalinity is the dominant anion in the river waters analyzed and in bulk of the samples it exceeds 70% of the TZ^-. The molar abundance of anions decrease as alkalinity>SO_4>Cl>NO_3>F except in the summer sample of the Aglar (RW99-10) and the spring waters (Kempti Fall and Shahashradhara) where SO_4>alkalinity. The SO_4 concentration exhibits a general increase from the upper to lower reaches. Rivers draining the crystallines in the upper reaches have SO_4 <100 μM whereas the Giri, Bata and Aglar, flowing through the Lesser Himalayan sediments which are reported to contain evaporites and black and gray shales (Valdiya, 1980) associated with pyrites, have >400 μM SO_4.

On a ternary anion diagram (Fig. 4.3), the data points fall along the alkalinity-(SO_4+Cl) line characteristic of carbonate-evaporite-sulphide weathering. The SO_4/Cl molar ratios in the YRS, though show a wide range, 0.7 to ~59 (average ~7), most of the values center around 3±2. Only 10 samples of 73 in the YRS, have SO_4/Cl>20. These samples are from the Aglar, *Tons* at Dehradun, the Giri and the Tons (after its confluence at Kalsi). The highest SO_4/Cl, 59 is in the June sample of Aglar which has also high values, 27 and 28 during October and September respectively. The significantly higher SO_4 relative to Cl is an indication that if evaporites are a major source of SO_4 to these waters, then their composition must be dominated by gypsum/anhydrite with only minor amounts of halite. Such a contention is supported by very high SO_4/Cl (4530) in the spring waters of Shahashradhara. In addition to evaporites, oxidative weathering of pyrites can also contribute SO_4 to the waters. Evaporite dissolution would supply Ca and SO_4 to the waters in the ratio 1:1. If SO_4 is also derived from H_2SO_4 generated via pyrite oxidation, it can result in SO_4/Ca>1. The observation that some of the rivers have SO_4≥Ca (Table 4.1) is an evidence for the supply of SO_4 to them by pyrite oxidation. Further, the evidence for oxidative weathering of pyrites throughout the YRS drainage basin is provided by significant positive correlation between Re and SO_4 in the YRS waters; which has been attributed to weathering of organic rich sediments containing high Re by sulphuric acid released from oxidation of pyrites which are generally associated with them (Chapter 5; Dalai et al. 2001a).

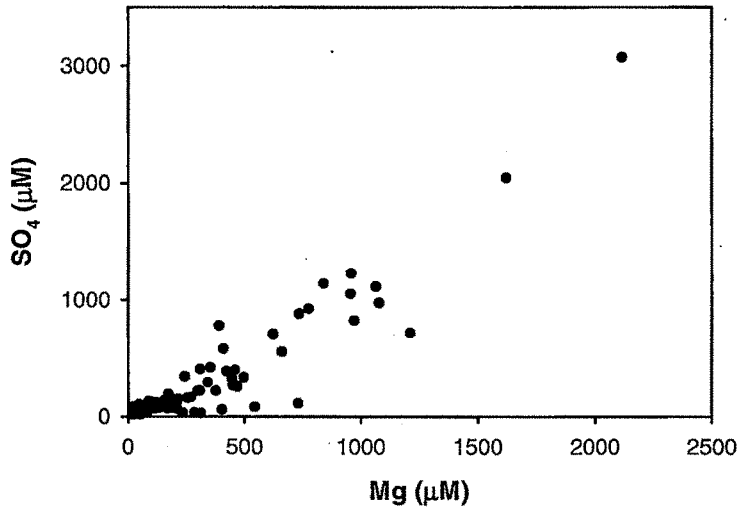

Fig. 4.10 Scatter plot of SO_4 vs. Mg in the YRS waters. A strong positive correlation is evident (r^2 = 0.85), a likely result of weathering of dolomites by sulphuric acid.

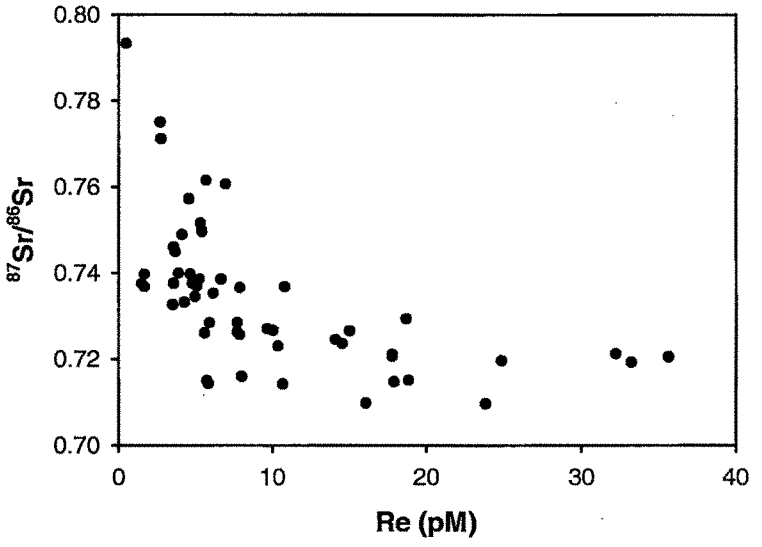

Fig. 4.11 Scatter plot of $^{87}Sr/^{86}Sr$ vs. dissolved Re in the YRS waters. An inverse trend suggests that weathering of lithologies associated with organic rich sediments contribute Sr with low $^{87}Sr/^{86}Sr$ to the YRS.

Other evidences in support of pyrite oxidation in the YRS drainage basin come from the positive correlation between Mg and SO_4 and the anticorrelation between $^{87}Sr/^{86}Sr$ and dissolved Re (Figs. 4.10 and 4.11). The correlation of Mg with SO_4 most likely results from weathering of dolomites by H_2SO_4. Similarly the inverse correlation between $^{87}Sr/^{86}Sr$ and Re can be understood in terms of weathering of organic rich sediments and associated pyrites

and carbonates/phosphates. The organic rich sediments contribute Re, and H_2SO_4 produced via pyrite oxidation release Sr from carbonates/phosphates with low $^{87}Sr/^{86}Sr$.

The NO_3 abundance generally centers around a few tens of μM, with lower values in the rivers draining the upper reaches (Table 4.1). The Yamuna samples from Saharanpur and its tributaries Asan, Giri, Bata all have higher NO_3 concentration, with values exceeding 30 μM (Table 4.1). One of the sources of the nitrate to rivers is fertilizers (Berner and Berner, 1996). The impact of agriculture on NO_3 abundances in the YRS is difficult to assess, as our knowledge on the agricultural practices and fertilizer uses in the drainage basins of these rivers is very limited. However, Asan river samples which have the highest NO_3 (>100 μM, Table 4.1) and high chloride (>200 μM) abundances among all the rivers, anthropogenic contribution could be a concern. Collins and Jenkins (1996) observed that terrace agriculture and use of nitrogenous mineral fertilizers elevated the concentrations of NO_3 and base cations in the streams draining the Middle Hills of the Nepal Himalaya.

Fluoride concentrations in the YRS are quite low, ~2 to 18 μM with a mean 9±3 μM, with no discernible trend along their course. They are in general lower than those in the Ganga headwaters (Sarin et al., 1992) and similar to those in the rivers draining the Nepal Himalaya and the Ganga-Brahmaputra in Bangladesh (Galy and France-Lanord, 1999).

4.2.2 Sources of major ions in the YRS

Major ions are supplied to rivers via atmospheric deposition, chemical weathering of various lithologies in the basin and anthropogenic sources. The dissolved concentrations of major elements and their ratios in the rains and streams/rivers of the YRS are examined, with suitable assumptions, to constrain the contributions from these sources. These results are used to derive silicate and carbonate weathering rates in the YRS basin and associated CO_2 consumption.

Considering that the YRS in the Himalaya is reasonably "pristine" and "remote" from thickly populated areas (particularly in its middle and upper reaches), anthropogenic contribution to its major ion budget is unlikely to be of importance. The impact of atmospheric deposition on the dissolved load can be gauged from the chemical composition of rain and snow in the region. Generally sea salt aerosols and atmospheric dust are the dominant sources of major ions to rain and snow in basins such as the YRS which are remote. In this study, three individual rainwater samples were collected from Dehradun and

analyzed for their major ions (Table 4.4). Of these, one sample (#3, Table 4.4) had a significant amount of particulate matter, this sample also has much higher concentrations of major ions compared to the other two samples. It seems likely that the particulate matter may have contributed to the high dissolved load in this sample and therefore it may not represent a "typical" rain sample of the region. Therefore, the data of this sample is not considered in the following discussions. Precipitation samples could not be collected from the upper reaches of the YRS, however, data are available for snow and ice samples from the Chhota Shigri (altitude: 4000-5600 m. latitude: 32°19'N, Nijampurkar et al., 1993) and Pindari glaciers (altitude: 3600-5720 m, latitude: 30°16' to 30°19'N, Pandey et al., 2001). These glaciers are located in the same range of altitude (~3300-6300 m) and latitude as the Yamunotri glacier.

Table 4.4 Chemical composition of rain, snow and glacier ice (μM)

Sample	Na	K	Ca	Mg	Cl	NO_3	SO_4	Ref.
Rain 1	0.2	0.8	0.7	0.4	3.2	—	4.5	1
Rain 2	0.2	0.8	1.3	0.7	3.8	—	4.8	1
Rain 3	1.7	7.3	65	6	13	61	47	1
Chhota Shigri (snow)	14	7	6	4	21	8	2	2
Chhota Shigri (ice)	8	3	2.6	1.4	11	7	1.8	2
Dokriani Bamak (snow)	10	3.4	4.2	2.4	19	3.4	6.8	3

1: This study, 2: Nijampurkar et al. (1993); 3: Sarin and Rao (2001)

It is seen from the data in Table 4.4 that among the major ions, atmospheric deposition can be important as a source only for chloride in the YRS. The chloride concentration in rain is ~5 μM and that in the snow/ice is ~20 μM compared to 5.7-256 μM in rivers and streams (Table 4.1). As bulk of the rivers in the YRS have >30 μM chloride, rainwater contribution of chloride to the YRS in general is <15 %. In a few streams, however, chloride is quite low <10 μM (Table 4.1), in these cases much of the Cl can be of atmospheric deposition. The inference that the atmospheric deposition of chloride is <15 % in bulk of the river samples, suggest that dissolution of halites is the major source of chloride to these rivers.

The contribution of Na to rivers/streams from atmospheric deposition can be estimated from Na/Cl ratios in rains/snow, which is ~0.5 (Table 4.4). Using this value, the Na contribution from atmospheric deposition is calculated to be, on average, <5% of its

concentration in rivers. K concentration in rains is <1 μM and that in the snow/glacier is ~3 μM (Table 4.4). This is less than ~15 % of its abundance even in the Amlawa river, which has the lowest K among all the rivers analyzed (Table 4.1). Ca and Mg in rainwater and snow/glacier samples are negligibly small (Table 4.4) to be of any significance to their river water budget.

(i) Silicate weathering

One of the main goals of this work, as mentioned earlier, is to constrain contemporary silicate and carbonate weathering rates in the Yamuna River Basin in the Himalaya. This goal can be achieved if the contributions of major cations to the rivers and streams of the YRS via silicate and carbonate weathering can be determined. Na in the waters is derived from cyclic salts, halite dissolution and silicate weathering, whereas the dominant source of K is silicates. Using Cl as an index of cyclic salts and halites, the silicate component of Na can be estimated as

$$Na_s = Na_r - Cl_r \text{ and } K_s \approx K_r$$

where the subscripts s and r refer to 'silicate' and 'river' respectively (Na_s is same as Na*). Bulk of the Na in the YRS, as mentioned earlier, is derived from silicate weathering. This, coupled with the observation that the YRS waters have measurable quantities of K and SiO_2, suggests that silicate weathering is an ongoing process in the basin. In estimating Na_s, it is assumed that the contribution of Na from carbonates is negligible. The Na/Ca molar ratio in Precambrian carbonates of the Krol Group is ~0.002 (Mazumdar, 1996). Given the Ca concentration in the YRS rivers range from ~90 to 2360 μM (Table 4.1), the Na contribution from these carbonates would be 0.2 to 4.7 μM. These values are much lower than the Na abundance in the rivers. Further, it is likely that Na in these carbonates is associated with silicates which are contained in them.

Rivers derive their Mg from carbonates and silicates whereas sources for Ca are carbonates, evaporites, silicates and minor phases such as phosphates. Apportionment of dissolved Ca and Mg (particularly Ca) among their various sources is more difficult because of uncertainties associated with the end member values and assumptions pertaining to their nature of release during weathering (Krishnaswami et al., 1999). Inspite of this, as discussed below, useful limits on silicate weathering contribution to the dissolved budgets of Ca and Mg in the YRS can be made.

The silicate component of Ca and Mg (Ca_s, Mg_s in moles ℓ^{-1}) can be derived as:

$$(Ca)_s = Na_s \times (Ca/Na)_{sol}$$

$$(Mg)_s = Na_s \times (Mg/Na)_{sol}$$

where $(Ca/Na)_{sol}$ and $(Mg/Na)_{sol}$ are the molar ratios released to river waters from the silicates in the drainage basins during their chemical weathering. The reliability on $(Ca/Na)_{sol}$ determines the uncertainties associated with Ca_s (and Mg_s) estimates. Krishnaswami and Singh (1998) and Krishnaswami et al. (1999) used values of 0.7±0.3 and 0.3±0.2 for $(Ca/Na)_{sol}$ and $(Mg/Na)_{sol}$ ratios. This compares with values of 0.5 and 0.2 respectively for $(Mg/K)_{sol}$ and $(Ca/Na)_{sol}$ used by Galy and France-Lanord (1999) for estimating the silicate contribution of Ca and Mg to the rivers in the Nepal Himalaya. (The $(Ca/Na)_{sol}$ ratio used by Galy and France-Lanord (1999) is based on (Ca/Na) in whole rock silicate composition of the Higher Himalaya (HH) and Lesser Himalaya (LH) and in plagioclase of the HHC, whereas the value of Krishnaswami et al. (1999) is based on (Ca/Na) in LH granites/gneisses, soil profiles and in rivers draining predominantly silicates. Among these, the Ca/Na in rivers is generally much higher than those in the granites/gneisses and those based on soil profiles resulting in a higher $(Ca/Na)_{sol}$). Bulk of the drainage basin of the YRS lies in the Lesser Himalaya. The average (Ca/Na) molar ratio in granites and gneisses of the LH is 0.46±0.28 (Krishnaswami et al., 1999). This is marginally higher than the value of 0.32±0.29 in HH crystallines (Krishnaswami et al., 1999). Granites from Hanuman Chatti (Table 4.2) and Sayana Chatti (Biyani, 1998) in the Higher Himalaya have Ca/Na, 0.15±0.13, which is within errors of those for the HH crystallines. (Ca/Na) in the bed sediments of the YRS (having no carbonate, Table 4.2) is 0.44±0.14. If river waters receive Ca and Na from these rocks in the same proportion as their abundance, then the $(Ca/Na)_{sol}$ would be in the range of 0.15-0.46. The Ca/Na* in Jola Gad (tributary of the Ganga), Didar Gad (tributary of the Yamuna) and Godu Gad (tributary of the Tons), flowing primarily through silicate terrains, are in the range of 1.15-1.6. These ratios are much higher than those in the silicate rocks, probably because of contribution of Ca to waters from carbonates and evaporites. Thus, based on data on the granites/gneisses of LH and HH, soil profiles in the LH and selected rivers Krishnaswami et al. (1999) used a value of 0.7±0.3 for $(Ca/Na)_{sol}$. In the present work, this value is used for estimation of Ca_s in the YRS. In addition, calculations are also made using $(Ca/Na)_{sol}$ = 0.35±0.15, similar to those observed in rocks. Similarly for $(Mg/Na)_{sol}$ a value of 0.3±0.2 has

been used. This value is based on the Mg/Na in LH crystallines (0.65±0.45), HH crystallines (0.31±0.28), granites from Hanuman Chatti and Sayana Chatti (0.15±0.08) and bed sediments with no carbonate (0.51±0.16).

From these values, the fraction of cation contributions from the silicates to the rivers, $(\Sigma Cat)_s$, can be calculated as:

$$(\Sigma Cat)_s = \frac{\Sigma(X_i)_s}{(\Sigma Cations)_r} = \frac{(Na_s + K_r + 0.7 \times Na_s + 0.3 \times Na_s)}{(Na_r + K_r + Mg_r + Ca_r)}$$

$(\Sigma Cat)_s$ in the YRS range from ~7 to 63% (molar) with an average of (25±11)%. It is important to observe that by decreasing the $(Ca/Na)_{sol}$, from 0.7 to 0.35, the range and average of $(\Sigma Cat)_s$ decreases marginally, 6 to 54% and (22±10)%. The distribution $(\Sigma Cat)_s$ estimated using 0.7 and 0.35 as $(Ca/Na)_{sol}$, is shown in the Fig. 4.12. As expected, the streams flowing mainly through silicate lithology, the Godu Gad and Didar Gad, have the highest silicate cation contributions, 54-63% and 42-47% respectively for summer and post monsoon periods using 0.7 and 0.35 as $(Ca/Na)_{sol}$. $(\Sigma Cat)_s$, in general, is higher in the tributaries of the Yamuna and Tons in the upper reaches where they drain predominantly crystallines. $(\Sigma Cat)_s$ are the lowest in the spring waters of Kempti Fall and Shahashradhara, ~0.5-3 %. Interestingly, $(\Sigma Cat)_s$ in the Yamuna at Batamandi and Saharanpur, where the river carries an integrated signature of weathering contributions from its entire basin in the Himalaya, is 20-28 %, suggesting that the calculated average of $(\Sigma Cat)_s$ in the YRS basin is reliable and not biased by sampling (or exclusion) of particular streams. The calculated $(\Sigma Cat)_s$, using two values of $(Ca/Na)_{sol}$, translates to 2.5 and 20.5 mg ℓ^{-1} of silicate cations in various rivers and ~1 to13 % wt. of TDS, during three seasons. The $(\Sigma Cat)_s$ in the Ganga waters at Rishikesh, based on the data in Table 4.1, is ~19-27 %. This compares well with the $(\Sigma Cat)_s$ estimate made earlier in the Ganga water at Rishikesh, 21-30 % (Krishnaswami et al., 1999).

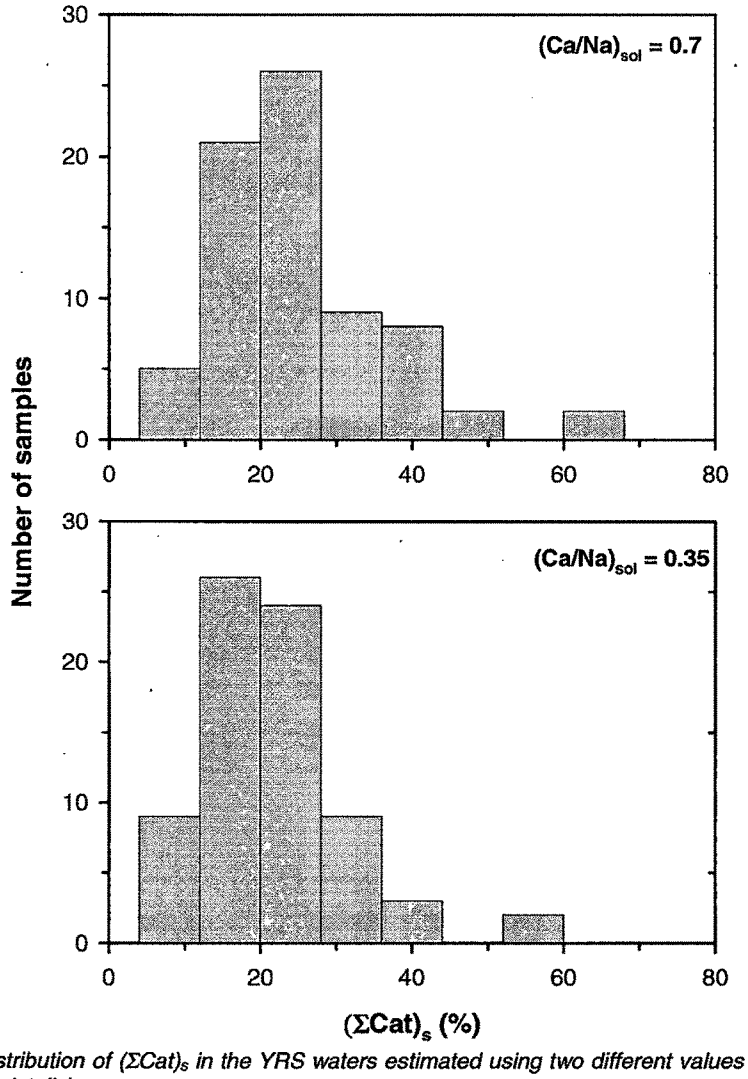

Fig. 4.12 Distribution of $(\Sigma Cat)_s$ in the YRS waters estimated using two different values of $(Ca/Na)_{sol}$ (see text for details).

$(\Sigma Cat)_s$ estimates for the YRS rivers show that in monsoon samples, with a few exceptions, they are either equal to or higher than those in the summer and post-monsoon samples (Fig. 4.13) Exception to this trend are the samples from the Yamuna at Rampur Mandi and the river Bata. This observation can result due to exposure of fresh silicate minerals by physical erosion during high water flow and their consequent weathering. This contention is supported by the observation that in many of the streams $^{87}Sr/^{86}Sr$ is higher during the monsoon period (see section 4.2.3). This result, however, differs from that

reported by Krishnaswami et al. (1999). This may be because their inference was based on samples collected during different years.

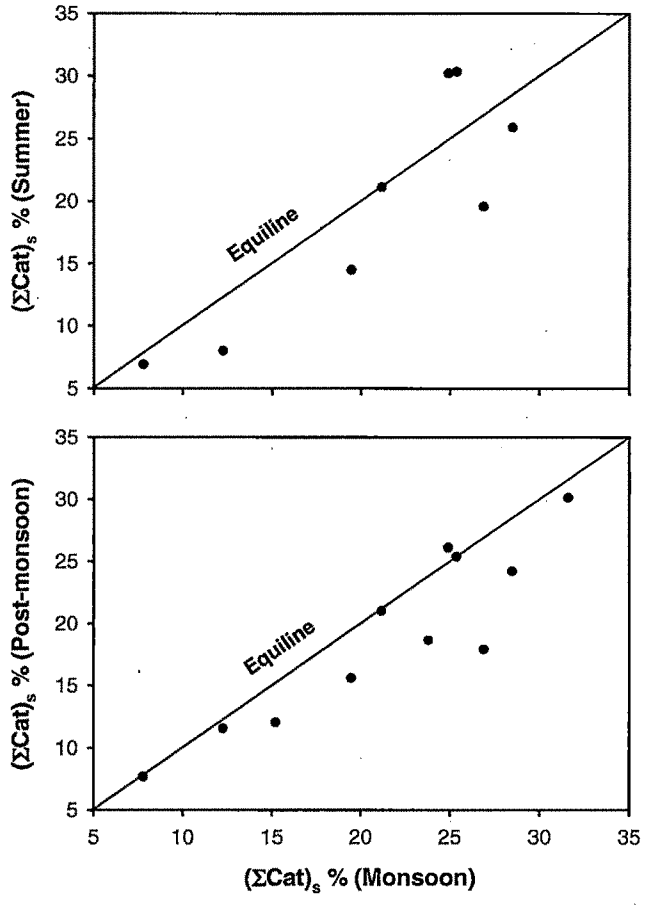

Fig. 4.13 Seasonal variation of $(\Sigma Cat)_s$ in the YRS waters. In general, monsoon samples have higher $(\Sigma Cat)_s$ than those collected during summer and post-monsoon.

Independent approach to gauge the intensity of aluminosilicate weathering in the catchment is from the Si/(Na*+K) ratios in river waters and values of chemical index of alteration of river sediments. The Si/(Na*+K) ratio is dependent on different silicate weathering reactions occurring in the basin. For example, Na-feldspar weathering to beidellite would yield a value of 1.7 for Si/(Na*+K) in the waters whereas K-feldspar weathering to kaolinite would give a ratio of 3 (Huh et al., 1998). The dissolved Si/(Na*+K) in the YRS varies from ~0.5 to 3.0 with an average ~1.2. The low average value of the ratio

in the YRS indicates that silicate weathering is not intense in the basin. Major ion data on the bed sediments (Table 4.2) support such an inference.

A measure of the degree of chemical weathering of these sediments can also be obtained from their Chemical Index of Alteration (CIA):

$$CIA = ([Al_2O_3]/[Al_2O_3+CaO^*+Na_2O+K_2O]) \times 100$$

where CaO^* represents Ca in the silicate fraction (Nesbitt and Young, 1982). During silicate weathering cations are released to solution depending on their solubility. For unweathered granites the CIA values would fall in the range of ~45-55, whereas in soil profiles generated by extensive weathering (as evident from their very low Na, Ca and K abundances) would yield a CIA of ~100. Similarly, unaltered albite, anorthite and K-feldspar have CIA ~50, 30 to 45 for fresh basalts and kaolinites close to 100 (Nesbitt and Young, 1982). In this study, bed sediments (sieved to <1 mm size and powdered to -100 mesh) from the YRS have been analyzed. CIA for the YRS sediments vary from ~51 to 69 with an average of ~60. (These values are uncorrected for any contribution of Ca from phosphates. Further, carbonates in the YRS catchment consist of both limestones and dolomites, with an average Ca/Mg wt. ratio 2.9 (Singh et al., 1998). Using this Ca/Mg ratio in the bed carbonates, the CIA for individual samples would be marginally lower, yielding an average ~59). In general, CIA for the YRS sediments in the lower reaches are higher suggesting relatively enhanced weathering in this region. This is expected as vegetation, soil CO_2 and temperature are relatively higher in the lower reaches. Furthermore, in these regions the contact time of water with the minerals is likely to be longer as they have shallower gradient than the upper reaches. The average CIA value in the YRS sediments is low and less than those in average shale (70-75) indicating that chemical weathering of silicates in the Yamuna basin in the Himalaya is not intense, consistent with the inference drawn earlier from Si/(Na*+K) in the waters. Ahmad et al. (1998) reported low values of CIA in the Indus bed (48-52) and suspended sediments (60-65) and concluded that mechanical erosion and weathering dominate their chemistry. In a region under active tectonic activity such as the YRS basin, with steep gradient and monsoon climate, physical erosion is likely to be more dominant than chemical weathering.

(ii) Carbonates and evaporite weathering

Carbonate is a major lithology in the drainage basin of the YRS, especially in the Lesser Himalaya (Fig. 2.3). The Precambrian carbonates which are widely exposed in the

drainage basins of the Yamuna, Tons and many of their tributaries such as Barni Gad, Shej Khad, Giri, Aglar are made of both calcites and dolomites (Singh et al., 1998; Valdiya, 1980). Evaporites are also reported to occur as pockets in the Krol carbonates in the drainage basins (Valdiya, 1980), however, their areal coverage and abundance are not well documented. Considering that both these lithologies can be weathered far more easily than silicates, they are expected to contribute significantly to the major ion budget of the YRS. The major ion abundances indeed support such a contention. Carbonate alkalinity and Ca are the major anion and cation in the YRS, with Ca, on an average, balancing ~70% of the alkalinity (Fig. 4.14a). This is a strong indication of dominance of carbonate weathering in the catchment. (Ca+Mg) exceed the alkalinity (Fig. 4.14b), but by and large balance (SO_4+alk) (Fig. 4.15), and together they account for 95% of the major ions (Table 4.1). This can be interpreted in terms of supply of these ions through weathering of Ca and Mg carbonates (and other phases such as phosphates) by H_2CO_3 and H_2SO_4 as well as supply of Ca and SO_4 via dissolution of gypsum/anhydrite. Evidence for pyrite oxidation in supplying H_2SO_4 for weathering of carbonates is seen in excess (or near equivalence) of SO_4 over Ca in a few samples and the significant correlation between Re-SO_4 (Chapter 5, Dalai et al., 2001a). Similarly, the strong linear correlation observed for Sr-SO_4 in these waters can result from the dissolution of evaporites (see later discussions on Sr). All these observations suggest that the cation and anion budgets of streams and rivers of the YRS is dominated by carbonate and evaporite weathering and pyrite oxidation, with the carbonates making larger contributions to the major ion balance. It is important to isolate the contribution of gypsum derived SO_4 from that via pyrite oxidation, as it has implications to the supply of protons for weathering and hence to CO_2 consumption. This is a difficult exercise to carry out in the YRS from the available major ion data and lithological information. It can, however, be inferred from the significant positive correlation between Mg and SO_4 in the YRS (Fig. 4.10) that carbonate weathering via H_2SO_4 exerts a dominant control on the SO_4 balance in these rivers. If all the SO_4 in the YRS is from oxidation of pyrites, then on average a fourth of the protons would be contributed by H_2SO_4 for weathering in the basin. Galy and France-Lanord (1999), in their studies of headwaters of the Narayani Basin in the Nepal Himalaya, observed that the primary source of sulphate in these waters is oxidation of sulphides.

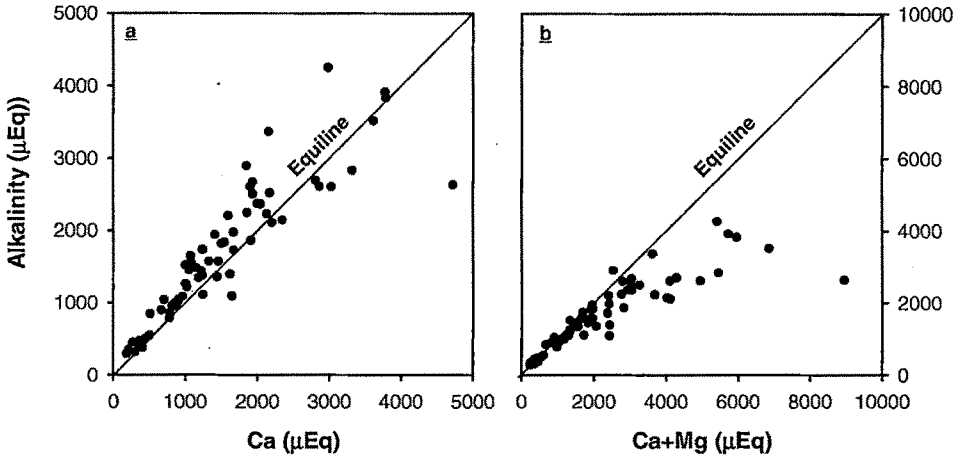

Fig. 4.14 Scatter plots of alkalinity vs. Ca (a) and Ca+Mg (b) in the YRS waters. Ca balances bulk of the alkalinity in the waters, Ca and Mg together exceed alkalinity requiring other anions to balance them.

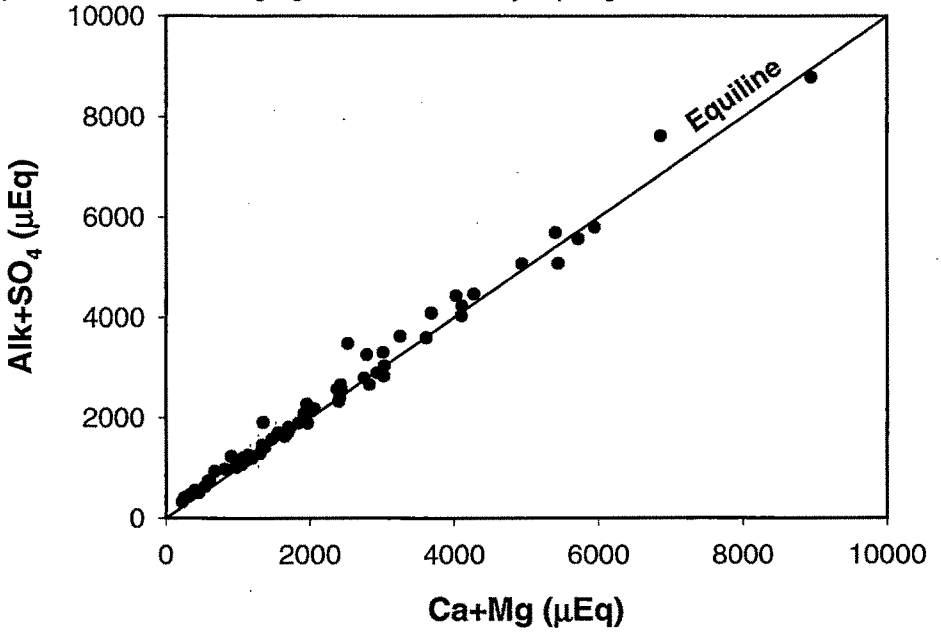

Fig. 4.15 Scatter plot of Ca+Mg vs. Alk+SO_4 in the YRS waters. The data by and large fall on the equiline, as the abundances of other cations and anions in the YRS rivers/streams are much lower.

An upper limit of carbonate contribution to the YRS cations can be derived as:

$$(\Sigma Cat)_{carb} = \frac{(Ca_r - Ca_s) + (Mg_r - Mg_s)}{(Na_r + K_r + Mg_r + Ca_r)}$$

In this calculation, it is assumed that Ca and Mg are contributed only from silicates and carbonates. This assumption is valid for Mg, however, for Ca it can overestimate the carbonate contribution as Ca can also be supplied to rivers via dissolution of gypsum (and

weathering of other phases such as phosphates). The calculated $(\Sigma Cat)_{carb}$ in the YRS range from ~32 to 91% , with a mean of 70±12% (for $Ca_s = 0.7Na_s$). These correspond to ~3-140 mg ℓ^{-1} of Ca+Mg in the YRS from carbonate weathering. A *lower limit* on the (Ca+Mg) supply from carbonates can be derived as:

$$(\Sigma Cat)_{carb} = \frac{\left[Ca_r - (Ca_s + Ca_{ev}) + (Mg_r - Mg_s)\right]}{(Na_r + K_r + Mg_r + Ca_r)}$$

Ca_{ev} (contribution of Ca from evaporites) is estimated assuming that all SO_4 in the YRS waters is from evaporites. This would yield a *lower limit* of Ca supply from carbonates. The calculated $(\Sigma Cat)_{carb}$ range from ~24 to 78% (mean ~50%), corresponding to ~2-63 mg ℓ^{-1} of Ca+Mg in the YRS [In six samples with $SO_4 \geq Ca$, after correction for Ca from silicates, estimated $(\Sigma Cat)_{carb}$ becomes negative, these have been excluded for the calculation of range and mean of $(\Sigma Cat)_{carb}$]. The calculation provides an *upper limit* of Ca supply to the YRS cations from evaporites (Ca_{ev}), this varies from ~3 to 55%, with a mean of ~20%. The cation balance in a few selected rivers is given in Table 4.5. These calculations assume that *all* SO_4 to be of evaporite origin and $(Ca/Na)_{sol}$ from silicate weathering is 0.7. The calculated carbonate Ca, therefore, is *lower limit* and evaporite Ca would be *upper limit*. It is seen from the results in Table 4.5 that Na and K in waters is dominated by contributions from silicate and Mg from carbonates. For Ca, carbonates are the major sources in most of the samples, in a few of them, however, evaporite contributions can be significant.

Table 4.5 Cation balance in selected streams of the YRS[a], percentage contributions.

Cations	Atmospheric/ Cyclic	Silicate	Carbonate	Evaporite
Yamuna@Hanuman Chatti (RW98-16)				
Na	6	55	1	32
K	4	96	0	0
Ca	0	7	64	29
Mg	0	11	89	0
(ΣCat)	*1*	*21*	*55*	*22*
Didar Gad (RW98-18)				
Na	13	83	1	0
K	6	94	0	0
Ca	0	21	67	12
Mg	0	34	66	0
(ΣCat)	*4*	*47*	*43*	*6*
Yamuna@Batamandi (RW98-4)				
Na	2	77	1	20

K	4	96	0	0
Ca	0	13	54	33
Mg	0	12	88	0
(ΣCat)	*0.4*	*24*	*54*	*21*
Yamuna@Saharanpur (RW98-33)				
Na	2	73	1	23
K	3	97	0	0
Ca	0	12	59	29
Mg	0	10	90	0
(ΣCat)	*0.4*	*22*	*58*	*19*
Tons@Mori (RW98-27)				
Na	7	70	1	16
K	4	96	0	0
Ca	0	17	49	34
Mg	0	39	61	0
(ΣCat)	*2*	*41*	*34*	*22*
Tons@confluence (RW98-32)				
Na	3	81	1	13
K	4	96	0	0
Ca	0	11	17	72
Mg	0	9	91	0
(ΣCat)	*0.5*	*21*	*36*	*42*

[a] Ca_{ev} is estimated assuming *all* SO_4 is derived from evaporites, and hence an *upper limit*. Ca_{carb} is a *lower limit*, as part of SO_4 (and Ca) also result via weathering of carbonates by sulphuric acid.

4.2.3 Dissolved Sr and $^{87}Sr/^{86}Sr$ in the YRS

The results on Sr and Ba concentrations and $^{87}Sr/^{86}Sr$ in the water samples are given in Table 4.1. The Sr concentration and $^{87}Sr/^{86}Sr$ in the YRS range between 120-13,400 nM and 0.7142-0.7932 respectively (Table 4.1). The Sr abundances in the Yamuna and its tributaries in the upper reaches are similar to those in the Ganga source waters, but in the lower reaches the tributaries of the YRS have more Sr. The rivers draining the northern slopes of the Himalaya, the Changjiang and Xijiang have similar Sr concentrations as those in the Yamuna in the lower reaches, however, the Mekong has higher Sr concentration (Gaillardet et al., 1999) than those in the Yamuna but similar to or lower than those in its tributaries in the lower reaches.

In general, the YRS streams in the upper reaches are more radiogenic in Sr isotopic composition than the ones in the lower reaches. The stream, Didar Gad, draining predominantly silicates (Fig. 2.9, Table 4.1) has the highest $^{87}Sr/^{86}Sr$ (0.7932). The spring waters of Shahashradhara have the highest Ca (~13,400 μM) and Sr (~62,000 nM) and low $^{87}Sr/^{86}Sr$ (0.7097). The $^{87}Sr/^{86}Sr$ in the YRS are similar to those reported in the Ganga headwaters (Krishnaswami et al., 1992), however, the tributaries of the YRS in the lower

reaches are less radiogenic than the Ganga source waters. $^{87}Sr/^{86}Sr$ in the YRS are in general higher than those in the Indus waters (Pande et al., 1994; Karim and Veizer, 2000), in rivers draining the basaltic terrains (Louvat and Allegre, 1997, Dessert et al., 2001) and much higher than the global river water average, 0.7119 (Palmer and Edmond, 1989). The rivers draining the northern slopes of the Himalaya have lower $^{87}Sr/^{86}Sr$ than those in the YRS.

The results of this study on Sr concentration and $^{87}Sr/^{86}Sr$ in the Ganga at Rishikesh and in the Yamuna at Saharanpur are compared with those available in the literature for the same locations (Palmer and Edmond, 1989; Krishnaswami et al., 1992, Table 4.6). The comparison shows that for both the Ganga and the Yamuna, there are measurable differences in Sr concentrations (±20%) and $^{87}Sr/^{86}Sr$ (0.2-0.3%) between the samples collected during the same season. These differences reflect inter/intra annual variations in the water properties.

Table 4.6 Comparison of Sr concentration and $^{87}Sr/^{86}Sr$ in the Ganga and the Yamuna: Present work and earlier reported values.

	Period	*Sr (nM)*	*$^{87}Sr/^{86}Sr$*	*Reference*
Ganga (Rishikesh)	Sept. 1982	580	0.7365	Krishnaswami et al. 1999
	Sept. 1999	507	0.73849	This study
	Nov. 1983	760	0.7408	Krishnaswami et al. 1999
	Oct. 1998	626	0.73856	This study
	Mar. 1982	800	0.7399	Krishnaswami et al. 1999
	June 1999	712	0.73657	This study
Yamuna (Saharanpur)	Mar. 1982	1360	0.7270	Palmer and Edmond, 1989
	June 1999	1664	0.72657	This study

$^{87}Sr/^{86}Sr$ in the Yamuna main channel seem to be primarily governed by the contributions from its tributaries. $^{87}Sr/^{86}Sr$ rises from 0.75158 at Hanuman Chatti to 0.75725 near Pali Gad Bridge (Table 4.1, Fig. 4.16), after Didar Gad and Jharjhar Gad, the tributaries with high radiogenic Sr composition, merge with the Yamuna. Downstream of Paligad Bridge, $^{87}Sr/^{86}Sr$ in the main channel decreases as tributaries with higher Sr concentration and lower $^{87}Sr/^{86}Sr$ merge. Lithology exerts a significant control on $^{87}Sr/^{86}Sr$ of the Yamuna along its course, the decrease in $^{87}Sr/^{86}Sr$ in lower reaches results mainly from contributions

from easily weatherable sedimentaries such as carbonates, evaporites and phosphates. These sedimentaries generally have wide range of Sr/Ca in them, with $^{87}Sr/^{86}Sr$ which overlap with each other but lower than those in silicates (Table 4.7). Evaporites and phosphates have higher Sr abundances compared to silicates and carbonates. The Sr/Ca in the Pc carbonates (Singh et al., 1998; Mazumdar, 1996) are lower than those in evaporites and phosphates (Table 4.7). The tributaries, the Aglar, the Giri, the Bata and the Asan, which drain these sedimentaries in the lower reaches, have high Sr and relatively low $^{87}Sr/^{86}Sr$. As these rivers merge with the Yamuna, its Sr concentration in the main channel increases with a consequent drop in $^{87}Sr/^{86}Sr$ (Fig. 4.16).

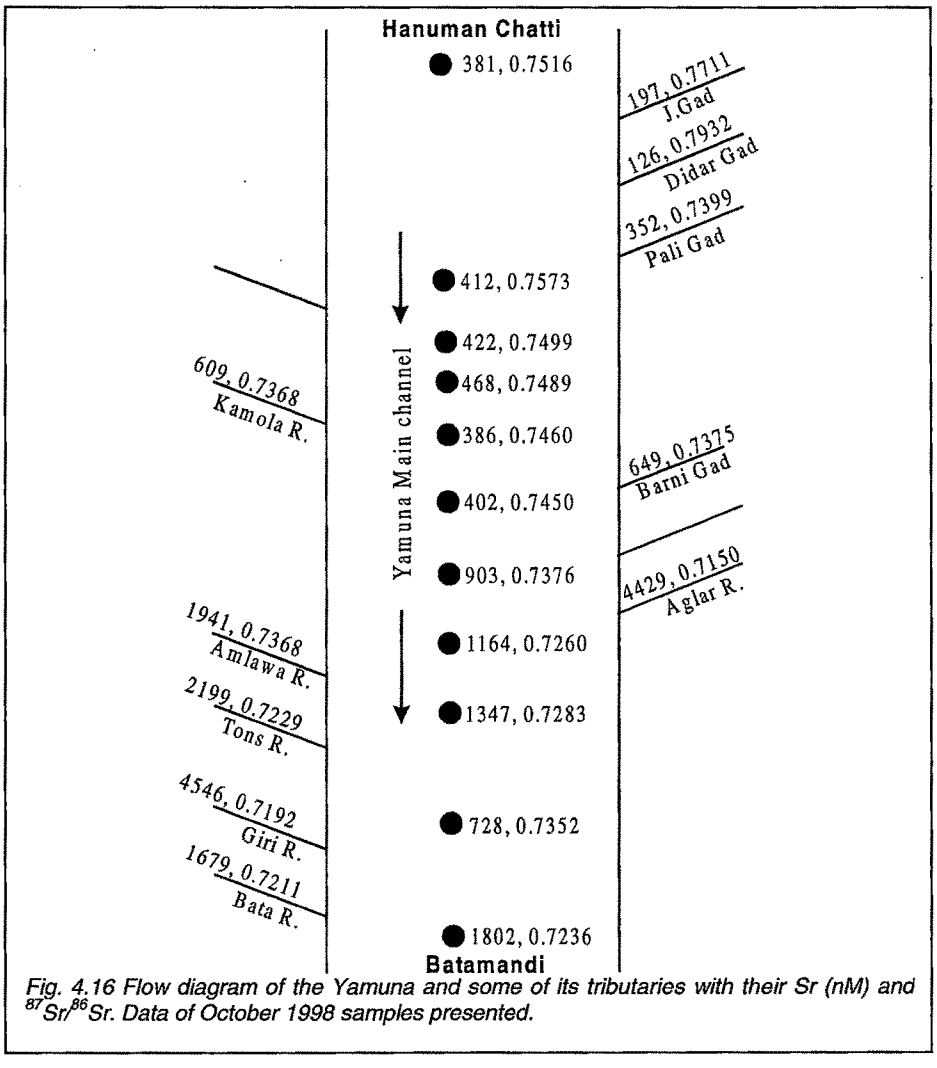

Fig. 4.16 Flow diagram of the Yamuna and some of its tributaries with their Sr (nM) and $^{87}Sr/^{86}Sr$. Data of October 1998 samples presented.

Table 4.7 Sr/Ca and $^{87}Sr/^{86}Sr$ in various lithologies

Lithology	Sr/Ca (nM/μM)	$^{87}Sr/^{86}Sr$
Crystallines	0.25	0.80[a]
Carbonates	0.20	0.7081-0.7162[b]
Evaporites	2.9[c]	0.7097[c]
Phosphorites	2.2[d]	0.7095-0.7124[e]

[a]from Krishnaswami et al. (1999). [b]for carbonates in the Yamuna catchment (Singh et al., 1998). [b]Sr/Ca based on data from Wedepohl (1978) and $^{87}Sr/^{86}Sr$ based on the data of spring waters of Shahashradhara. [d]data from Mazumdar (1996). [e]based on analysis of four phosphorite samples from Maldeota and Durmala mines as a part of this work.

Sr/Ca (nM μM^{-1}) in the YRS varies from 0.5 to 5.7 and average 1.6±0.9. In general, Sr/Ca in the streams/rivers are lower in the upper reaches and increase in the lower reaches. Sr abundances in the YRS show positive correlation with the Ca, Mg among the cations and alkalinity and SO_4 among the anions whereas $^{87}Sr/^{86}Sr$ vary inversely with all these properties (Table 4.8, Figs. 4.17-4.20). Similar trends are also seen with respect to TDS, this is expected as Ca, Mg, SO_4 and alkalinity make up >90% of TDS. Statistical analysis of Sr with these parameters (Table 4.8) shows that there is significant scatter around the best-fit lines, possibly indicating contributions from multiple end members. This might also be contributing to the intercepts observed for these lines (Table 4.8). Regression lines on plots of $^{87}Sr/^{86}Sr$ vs. 1/Ca and $1/SO_4$ have intercepts of 0.718 and 0.726 respectively (Table 4.8), higher than the $^{87}Sr/^{86}Sr$ for Pc carbonates in the YRS basin, evaporites and phosphorites (Table 4.7). Implications of these values would be discussed in latter sections.

Table 4.8 Interrelation of Sr, Ba and $^{87}Sr/^{86}Sr$ with major ions in the YRS.

Pair	*n*	*Slope*[a]	*Int.*	r^2
Sr-Ca	73	3.25	-903	0.66
Sr-Mg	73	4.29	-126	0.76
Sr-SO_4	73	3.67	192	0.90
Sr-TDS	73	12.12	-829	0.66
Ba-Sr	69	0.08	44	0.76
Ba-Ca	70	0.32	-59	0.81
$^{87}Sr/^{86}Sr$-1/Ca	50	8.15	0.718	0.80
$^{87}Sr/^{86}Sr$-1/SO_4	50	0.89	0.726	0.63

[a]nM μM^{-1} for regression of Sr and Ba with major ions, nM (mg ℓ^{-1})$^{-1}$ for Sr-TDS, nM nM^{-1} for Sr-Ba. Int.: intercept.

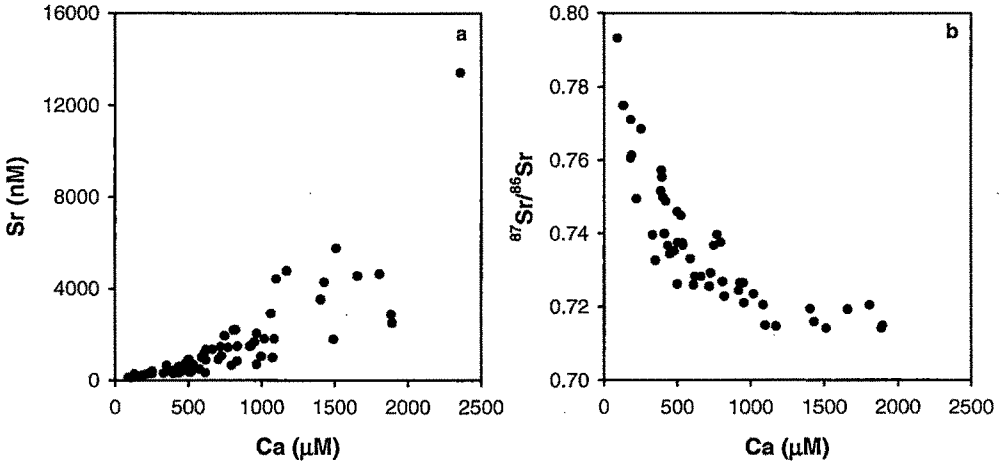

Fig. 4.17 Scatter plots of Sr (a) and $^{87}Sr/^{86}Sr$ (b) with Ca in the YRS waters. Sr derived from Ca rich lithologies such as carbonates, evaporites and phosphates dilute the radiogenic Sr isotopic composition of these waters.

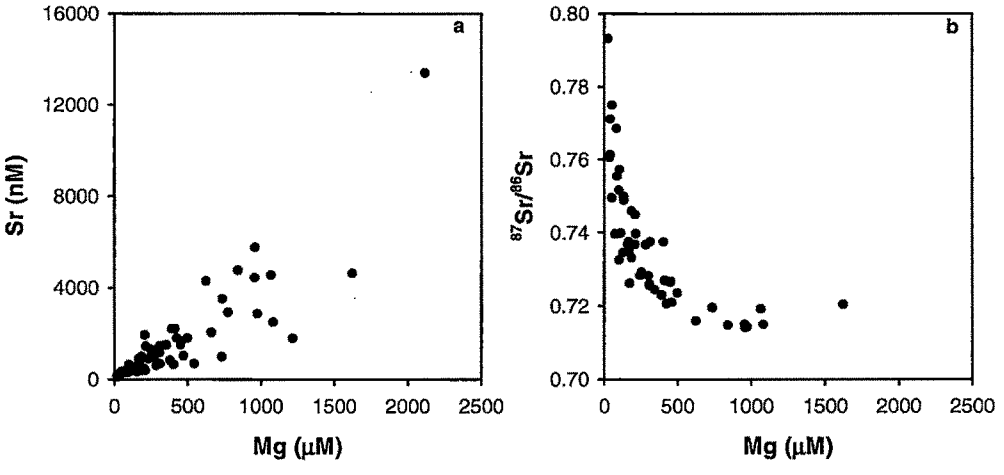

Fig. 4.18 Scatter plots of Sr (a) and $^{87}Sr/^{86}Sr$ (b) with Mg in the YRS waters. There exists a significant positive correlation between Sr and Mg (r^2=0.76). $^{87}Sr/^{86}Sr$ decreases with increasing Mg. Dolomite weathering contributes Mg whereas associated lithologies such as evaporites and phosphates seem to be contributing to Sr with low $^{87}Sr/^{86}Sr$.

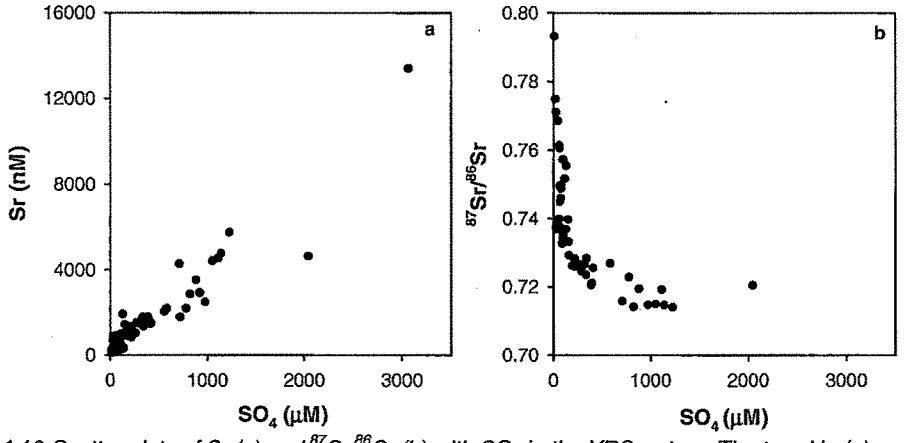

Fig. 4.19 Scatter plots of Sr (a) and $^{87}Sr/^{86}Sr$ (b) with SO_4 in the YRS waters. The trend in (a) can result from supply of Sr from evaporites. Weathering of sedimentaries by H_2SO_4 and evaporite dissolution play a significant role in influencing the Sr and its isotopic composition in the YRS (see text for detailed discussion).

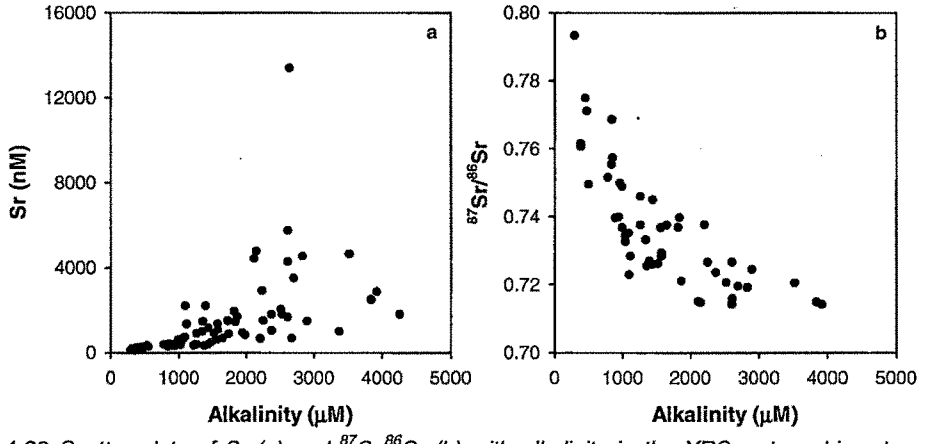

Fig. 4.20 Scatter plots of Sr (a) and $^{87}Sr/^{86}Sr$ (b) with alkalinity in the YRS waters. Limestone and dolomite weathering act as a diluent for the radiogenic Sr isotopic composition of the YRS rivers.

$^{87}Sr/^{86}Sr$ in the YRS covaries with SiO_2/TDS and $(Na^*+K)/TZ^+$ [Figs. 4.21a, b], both these ratios being measures of fraction of silicate contribution to the dissolved solids in rivers (Dalai et al., 2001b). Such covariations have implications to the source of Sr in rivers as discussed in the next section.

Sr abundances in the YRS and in the Ganga are generally lower during the monsoon than those during summer or post-monsoon (Table 4.1). In the Yamuna mainstream, $^{87}Sr/^{86}Sr$ during the monsoon season are in general higher (by 0.005 to 0.014) compared to post-monsoon (except at Rampur Mandi). The stream Godu Gad, draining predominantly silicates

has higher $^{87}Sr/^{86}Sr$ during post-monsoon (0.7750) compared to summer (0.7686). The tributaries in the lower reaches show no clear seasonal trend in their $^{87}Sr/^{86}Sr$.

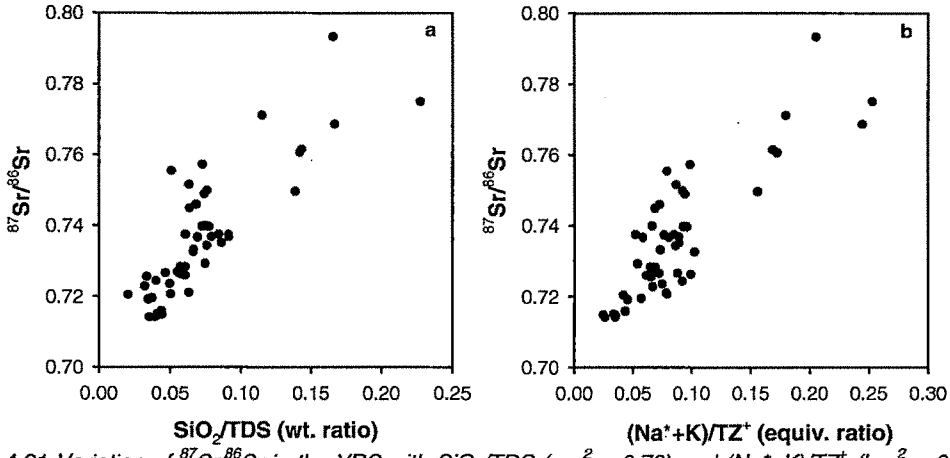

Fig. 4.21 Variation of $^{87}Sr/^{86}Sr$ in the YRS with SiO_2/TDS (a, r^2 = 0.70) and $(Na^*+K)/TZ^+$ (b, r^2 = 0.72). Positive trends of $^{87}Sr/^{86}Sr$ with these ratios (measure of silicate weathering) suggest that release of Na, K and Si to waters via silicate weathering is accompanied by an increase in $^{87}Sr/^{86}Sr$ of these rivers. The best fit lines yield intercept of 0.709 and 0.710, $^{87}Sr/^{86}Sr$ in the "non-silicate" components.

The Ganga at Rishikesh has higher $^{87}Sr/^{86}Sr$ during monsoon (0.7385) and post-monsoon (0.7386) than that during summer (0.7366). In the Yamuna at Saharanpur, $^{87}Sr/^{86}Sr$ remained the same during summer and post-monsoon (0.7266) while it decreased slightly during the monsoon (0.7262). These differences can be attributed to variability in weathering intensities of different minerals during various seasons and their mixing proportions in river. It is interesting to observe that in the Yamuna mainstream, an increase in $^{87}Sr/^{86}Sr$ in samples collected during monsoon is accompanied by a corresponding increase in silicate cation contributions $(\Sigma Cat)_s$ during this season. These trends further support the inference drawn earlier that during monsoon, exposure of fresh silicate mineral surfaces and their subsequent weathering occur in the YRS basin caused by rapid physical erosion.

4.2.4 Sources of Sr and their control on $^{87}Sr/^{86}Sr$

As already mentioned in the earlier sections, the YRS drains multilithological terrains comprising predominantly of crystallines, sedimentary silicates and carbonates, with minor amounts of evaporites, phosphates, black and gray shales. All these lithologies can contribute to the dissolved Sr of the YRS rivers/streams. One of the goals of this study is to constrain the relative contributions of Sr from these sources to the YRS and to assess their impact on

the riverine Sr isotopic composition. The co-variation of Sr with Ca, Mg, Na* and SO_4 (Figs. 4.17-4.20, 4.22), indicate that Sr in these waters can be derived from sources such as carbonates (Ca, Mg), silicates (Na*), evaporites (Ca, SO_4) and phosphorites (Ca) occurring in the catchment (Dalai et al., 2001c).

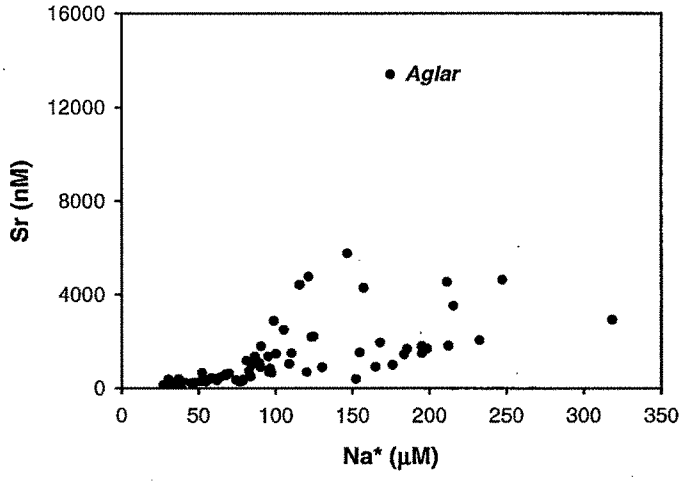

Fig. 4.22 Scatter plot of Sr vs. Na in the YRS waters. Sr shows an overall positive correlation with Na* though with significant scatter. The data fan out from a low Na*-Sr end member, indicative of multiple sources.*

In the YRS Na* and Sr though show an overall positive correlation (Fig. 4.22), the points fan out from low values suggesting Sr is derived from multiple sources. The river Aglar, as already mentioned, draining through the Krol carbonates might have a significant contribution of its Sr from evaporites which occur in these carbonates. Co-variation of $^{87}Sr/^{86}Sr$ with SiO_2/TDS and $(Na^*+K)/(TZ^+)^*$ (Figs. 4.21a, b) leads to infer that silicates dominate the high radiogenic Sr isotope end member of the YRS streams/rivers. This is further supported by the observation that the streams draining the crystallines in the Higher Himalaya have $^{87}Sr/^{86}Sr \geq 0.74$. The regression line plotted through the data (Figs 4.21a, b) have intercepts of 0.709 and 0.710, which is very similar to the average $^{87}Sr/^{86}Sr$ of Pc carbonates in the Yamuna basin (0.711), phosphates analyzed in this work (~0.711) and evaporites (based on the $^{87}Sr/^{86}Sr$ of Shahashradhara, 0.7097) supporting the idea that these lithologies are responsible for the low $^{87}Sr/^{86}Sr$ in the YRS rivers.

In a plot of 1/Sr vs. $^{87}Sr/^{86}Sr$, the data points fall by and large on a two end member mixing line with some scatter (r^2=0.84, Fig.4.23); indicating that as a first approximation, the

Sr abundance and $^{87}Sr/^{86}Sr$ in the YRS rivers may be considered as a mixture of two components, one with low Sr and high $^{87}Sr/^{86}Sr$ and the other with high Sr and low $^{87}Sr/^{86}Sr$. The intercept of the regression line, 0.719, is similar to observed intercepts in plots of $^{87}Sr/^{86}Sr$ vs. 1/Ca and $1/SO_4$ (Table 4.8) but marginally higher than the $^{87}Sr/^{86}Sr$ of Pc

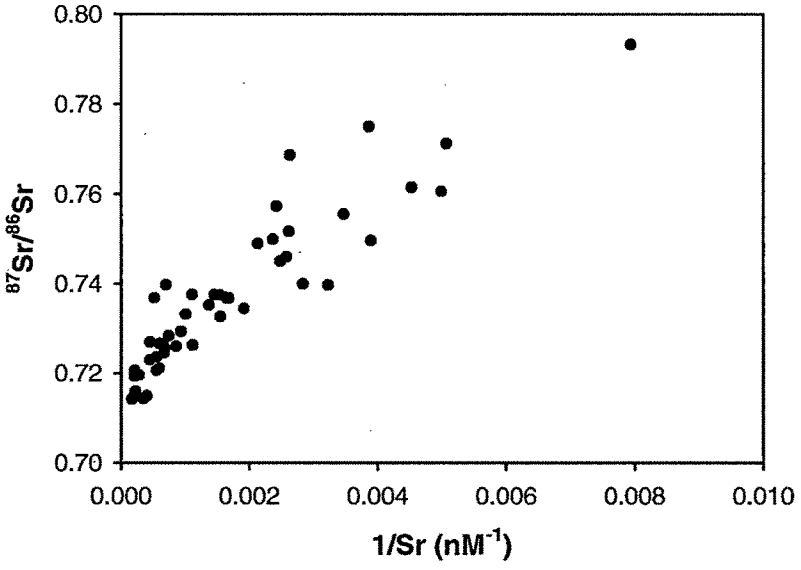

Fig. 4.23 Mixing plot of Sr and $^{87}Sr/^{86}Sr$ of the YRS waters. Samples by and large define a two component mixing trend (see text for discussion).

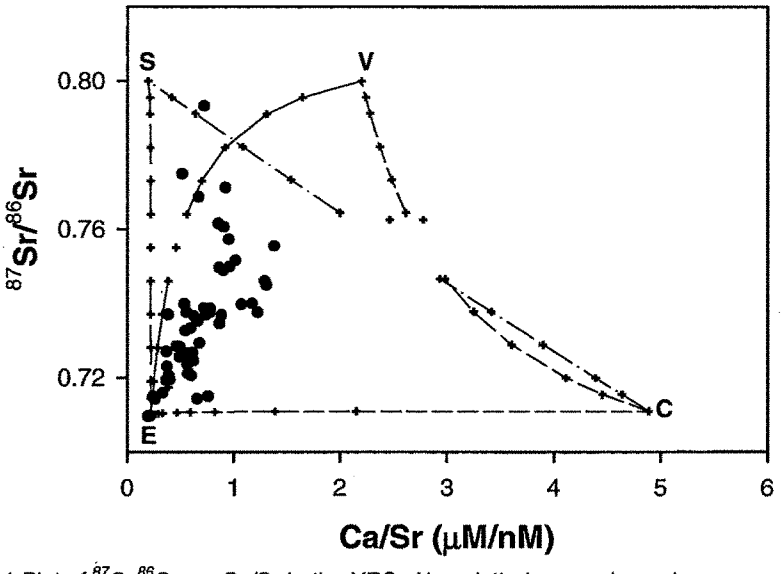

Fig. 4.24 Plot of $^{87}Sr/^{86}Sr$ vs. Ca/Sr in the YRS. Also plotted are end member compositions of silicates (S), Precambrian carbonates (C), evaporites (E) and vein-calcites (V). Sr and its isotopic composition in the YRS can be explained by mixing of carbonates, evaporites, silicates and/or vein-calcites (see text for discussion).

carbonates in the YRS basin (0.708-0.716), phosphorites (0.7095-0.7124) and evaporites (0.7097). A closer look at the data (Fig. 4.23) reveals the points fan out from (1/Sr) of ~10^{-4} nM^{-1} and $^{87}Sr/^{86}Sr$ of ~0.71, indicative of multiple end members. To resolve the various components contributing to Sr and its isotopes in the YRS better, Ca/Sr is plotted vs. $^{87}Sr/^{86}Sr$ (Fig. 4.24) as Ca/Sr vary significantly among the various lithologies (Table 4.7). In this diagram, vein-calcites are also plotted as an end member in addition to silicates, carbonates and evaporites. Recently, vein-calcites have been suggested as an important component in determining the $^{87}Sr/^{86}Sr$ of rivers draining the Himalaya (Blum et al., 1998; Jacobson and Blum, 2000). Silicates and vein-calcites may satisfy the high $^{87}Sr/^{86}Sr$ end member whereas carbonates, evaporites, phosphates all can be a part of low $^{87}Sr/^{86}Sr$ end member. Further, this plot shows the need for more than two components to account for the Sr and $^{87}Sr/^{86}Sr$ in the YRS.

Singh et al. (1998) based on a detailed analysis of Sr abundance and $^{87}Sr/^{86}Sr$ in Precambrian carbonates from the Lesser Himalaya, inferred that these carbonates are unlikely to be a major contributor to the high $^{87}Sr/^{86}Sr$ and Sr budget of the G-G-I source waters in the Himalaya on a basin wide scale. They arrived at this conclusion from the low $^{87}Sr/^{86}Sr$ and Sr/Ca ratios in carbonates relative to those in the river waters. The $^{87}Sr/^{86}Sr$ in Pc carbonates, sampled all across the Lesser Himalaya, average 0.725±0.043 and Sr/Ca 0.20±0.15 (Fig. 4.25, Singh et al., 1998). Bulk of these carbonates, however, have $^{87}Sr/^{86}Sr$ in the range of 0.706 to 0.732, with a few of them having values as high as ~0.89. This compares with the $^{87}Sr/^{86}Sr$ of 0.7142 to 0.7932 (mean: 0.736±0.018) and Sr/Ca of 0.5 to 5.7 (mean: 1.6±0.9) in the YRS (Fig. 4.25). In the Yamuna catchment, carbonates occurring in the inner belt (Chakrata-Tiuni-Deoban region) and outer belt (Dehradun-Mussoorie and Solan region) have a narrow range of $^{87}Sr/^{86}Sr$, 0.708-0.716, with a mean, 0.711±0.002. The spring waters of Kempti Fall have $^{87}Sr/^{86}Sr$ 0.7095, similar to that in carbonates collected near the fall (Singh et al., 1998). Out of 50 YRS river water samples analyzed, 44 have $^{87}Sr/^{86}Sr>0.716$ (Table 4.1), the maximum reported for Pc carbonates in the Yamuna catchment (Singh et al., 1998). Hence in most of these rivers/streams, sources in addition to Pc carbonates would have to be invoked to explain their high radiogenic $^{87}Sr/^{86}Sr$. For example, Shej Khad, the stream draining predominantly Pc carbonates of Deoban Formation (maximum reported $^{87}Sr/^{86}Sr$ 0.716), has $^{87}Sr/^{86}Sr$ 0.7293. The YRS rivers in the lower reaches; Aglar, Giri, *Tons* at

Dehradun and Asan, all have low $^{87}Sr/^{86}Sr$, 0.7142 to 0.7205. These rivers have a significant part of their drainage basins in carbonates of the inner and outer belts of the Lesser Himalaya (Fig. 2.3). It is tempting to infer from these observations that carbonate weathering could have a significant influence on their Sr isotopic composition.

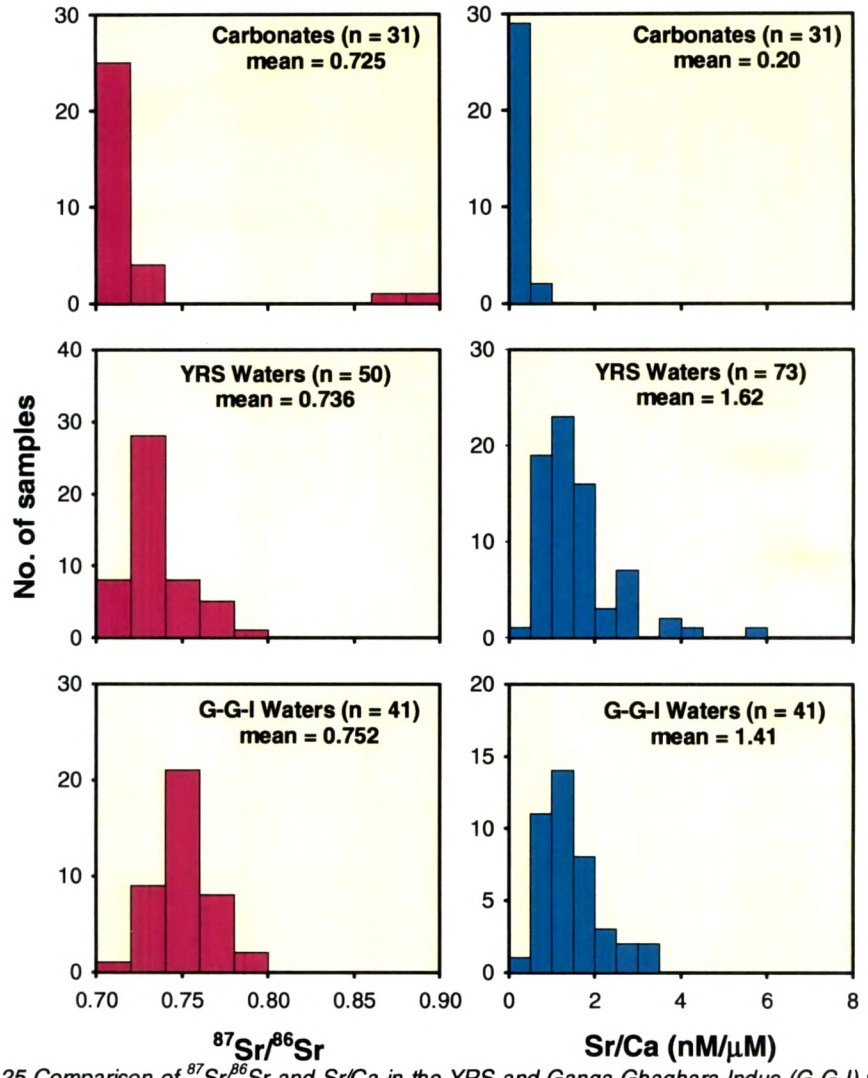

Fig. 4.25 Comparison of $^{87}Sr/^{86}Sr$ and Sr/Ca in the YRS and Ganga-Ghaghara-Indus (G-G-I) waters and Precambrian carbonates of the Lesser Himalaya. These carbonates have low $^{87}Sr/^{86}Sr$ and Sr/Ca compared to those in the river waters.

The role of carbonates as an important regulator of $^{87}Sr/^{86}Sr$ in these waters would also depend on their contributions to Sr budget. Estimates on this can be made from the Sr/Ca ratio of Pc carbonates and Ca concentrations of the rivers assuming that both Sr and Ca are released to waters in the same proportion as their abundances in the carbonates and that

they behave conservatively after their release to river (see latter section). There is a concern as to whether this requirement can be met, considering that many of the YRS river waters are supersaturated with calcite and the precipitation of calcite can enhance Sr/Ca in dissolved phase (English et al., 2000). As already discussed, it is unclear if precipitation of calcite occur in these waters. More work needs to be done to determine if calcite precipitation occurs from these waters and consequently elevates their Sr/Ca. Inspite of this uncertainty, it is evident that Precambrian carbonates is not a source for high $^{87}Sr/^{86}Sr$ of the YRS streams on a basin wide scale, as $^{87}Sr/^{86}Sr$ in most of the carbonates are ≤ 0.716. These carbonates, however, could become important on a local scale and for individual streams, if there are pockets of them with highly radiogenic Sr isotope composition such as those reported in Pithoragarh and Kanalichina (Singh et al., 1998). Such carbonates, however, have not been reported yet in the Yamuna basin. Further, as discussed in the next section, the contribution of Precambrian carbonates to the Sr budget of the YRS is estimates to be only ~15% on average.

Evaporites and phosphates are other lithologies, which can supply significant quantities of Sr to these waters with low $^{87}Sr/^{86}Sr$. Gypsum has been reported to occur as pockets in the Krol carbonates in the Lesser Himalaya (Valdiya, 1980). Phosphorites are known to be associated with black shales-carbonate sequences. However, the areal coverage and distribution of evaporites and phosphates in the YRS basin is not known. SO_4 is a major anion of YRS streams and account for ~2 to 35 % of anion abundance on a molar basis. SO_4 in rivers can be derived from both oxidation of pyrites and dissolution of evaporites. The strong correlation of Re and SO_4 in these waters has been attributed to ubiquitous pyrite oxidation in the drainage basin and suggests that it is an important source of SO_4 to the YRS waters (Chapter 5, Dalai et al., 2001a). This inference is drawn from the coexistence of pyrites with organic rich sediments, which are generally abundant in Re. Weathering of these sediments and pyrites release Re and SO_4 to rivers. The organic rich sediments are also often associated with carbonates and phosphorites e.g. black shales-carbonates-phosphates layers in Maldeota and Durmala phosphorite mines, near Dehradun. Weathering of these assemblage release Re, Ca, SO_4 and Sr to waters with low $^{87}Sr/^{86}Sr$. The strong correlation between Re and Sr and inverse correlation of Re and $^{87}Sr/^{86}Sr$ (Figs. 4.11, 4.26) very likely

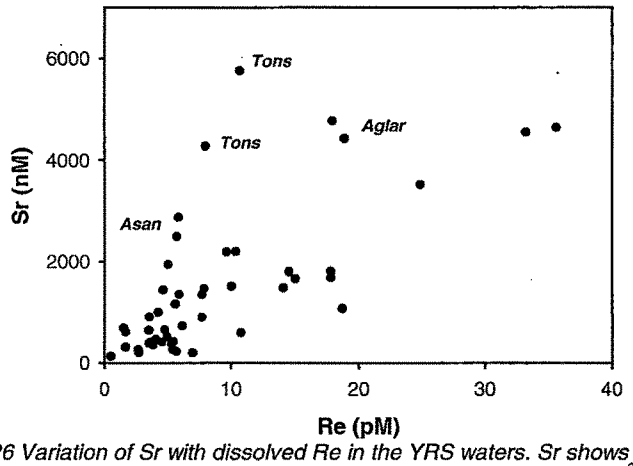

Fig. 4.26 Variation of Sr with dissolved Re in the YRS waters. Sr shows an over all increasing trend with Re though with considerable scatter. $^{87}Sr/^{86}Sr$ decreases with increasing Re (Fig. 4.11). These trends suggest that lithologies associated with Re rich sediments contribute Sr to the YRS waters with low $^{87}Sr/^{86}Sr$.

result from weathering of such multi-mineral assemblages. The scatter on Re-Sr plot supports the presence of multiple end members, fanning out from a low Sr, Re end member.

Sr mass balance in the YRS

As discussed earlier, the lithologies contributing to Sr of the YRS are silicates, carbonates, evaporites and phosphates.

Silicate contribution to the dissolved Sr load to the YRS can be estimated through the approaches outlined by Krishnaswami et al. (1999). In the first approach, it is assumed that Sr and Na in the silicates are released to solution in the same proportion as their abundance. Sr/Na (nM/μM) in the LH granites/gneisses average 1.68±0.72 (Krishnaswami et al. 1999). Granites occurring around the source region of the Yamuna, from Sayana Chatti (Biyani, 1998) and Hanuman Chatti (this study, Table 4.2) have an average Sr/Na 0.93±0.22, which is lower but overlaps within errors, with the LH average. Based on Sr/Na on soil profiles (Gardner and Walsh, 1996) developed on metamorphics in LH, Krishnaswami et al. (1999) estimated that Sr/Na released to the solution from silicate source rocks could range between 2.5-2.9. Another approach to assess the Sr/Na released to the waters from silicates is from the chemistry of streams flowing predominantly through silicate lithology. Among the rivers sampled, Godu Gad, with the lowest Ca/Na, SO_4/HCO_3 and high $^{87}Sr/^{86}Sr$ (0.77495) meets this requirement. It has Sr/Na* 2.48, which is the lowest among all the rivers analyzed in this study. These exercises, thus indicate that Sr/Na released to the rivers from silicate

weathering, $(Sr/Na)_{sol}$ can range between 1.0-2.9. For calculation of silicate contribution to the Sr load in the rivers, a value of 2.0±0.8 for $(Sr/Na)_{sol}$ is used, this is same as that used by Krishnaswami et al. (1999).

The silicate Sr contribution to the YRS (Sr_s) is calculates as:

$$Sr_s = (Sr/Na)_{sol} \times Na^*$$

where Na* is the sodium corrected for cyclic contributions, Na* = Na-Cl. The calculated values of Sr_s varies between ~55 to 640 nM, ~3 to 80% of the total dissolved Sr. It is seen that in the YRS streams/rivers, fraction of Sr derived from silicates decreases with increase in their Sr concentration (Fig. 4.27) resulting from contributions from components with high Sr such as evaporites and phosphates.

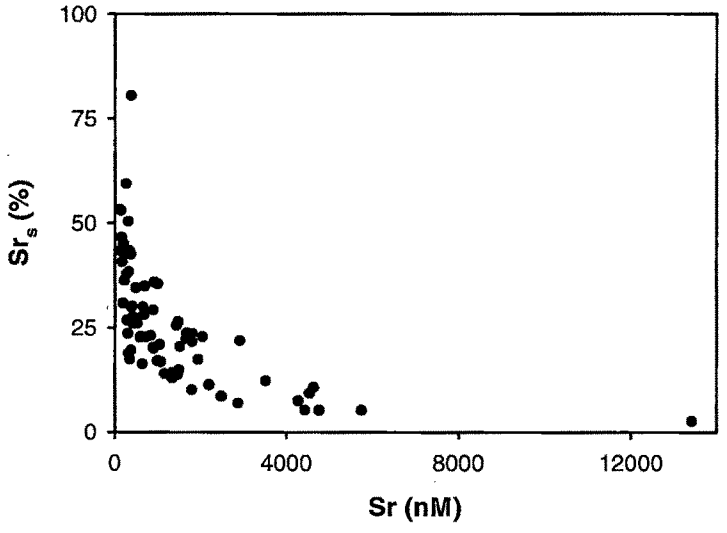

Fig. 4.27 Variation of Sr_s with Sr abundances in the YRS streams. Sr_s decreases with increase in Sr.

The average of Sr_s estimates for all the YRS streams analyzed in this study is 26±15%. Sr_s values for the Yamuna at Batamandi at the foothills of the Himalaya where the Yamuna integrates the Sr contributions from its entire catchment upstream varies from 22 to 26% for the three different sampling periods. The similarity in the average Sr_s value derived for all streams and that for the Yamuna at Batamandi lends further support to the estimate of 26% as the representative average silicate Sr contribution in the YRS. In the Yamuna at Hanuman Chatti, Sr_s constitute 20-27 percent of total Sr. In the streams Didar Gad and Godu

Gad, flowing mainly through silicates, Sr_s ranged from 43-53% and 53-81% respectively. Sr_s in the Ganga at Rishikesh is ~23%. The spring waters, as expected, have lower Sr_s in them, 0.1-0.3% for Kempti Fall and 0.9% for Shahashradhara. Using the lower and upper limits of $(Sr/Na)_{sol}$, 1.2 and 2.8, Sr_s in the YRS average at 16±9% (range 2-48%) and 36±20% (range 4-100%) respectively.

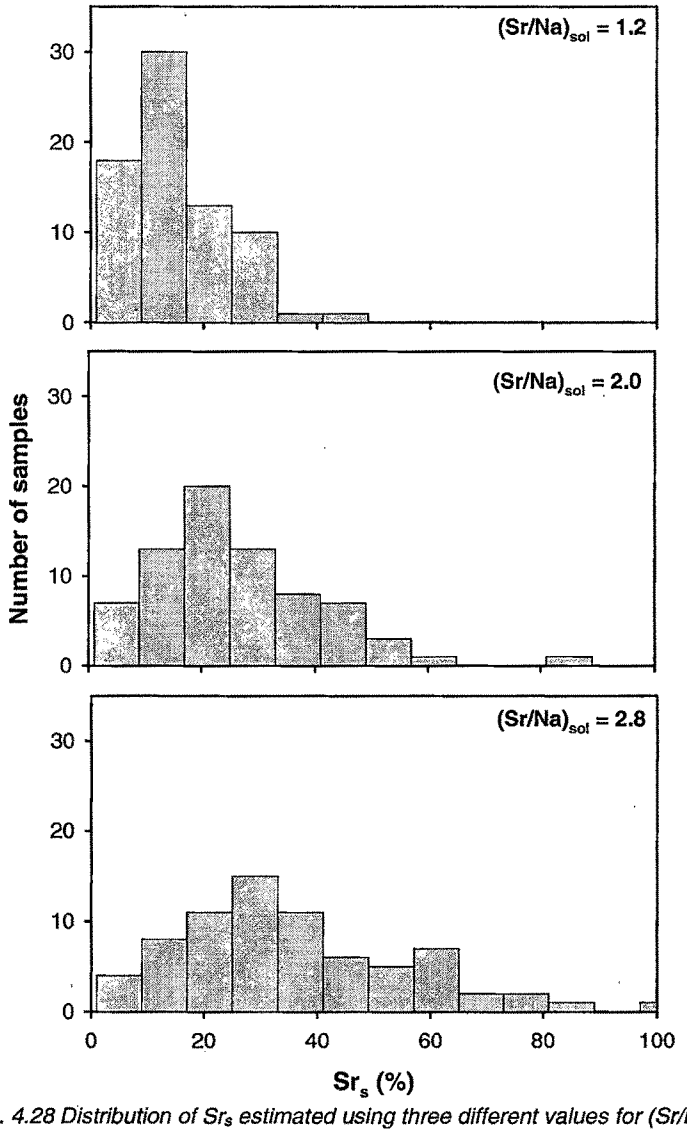

Fig. 4.28 Distribution of Sr_s estimated using three different values for $(Sr/Na)_{sol}$.

The distribution of Sr_s in the rivers calculated using three different values for $(Sr/Na)_{sol}$, 1.2, 2.0 and 2.8 are shown in Fig. 4.28.

Sr_s shows a significant positive correlation with $^{87}Sr/^{86}Sr$ (Fig 4.29) suggesting that silicate weathering in the catchment exerts a dominant control on the radiogenic composition of the rivers in YRS. The intercept of the regression line, 0.713, is very similar to the $^{87}Sr/^{86}Sr$ of non-silicate end members. A similar correlation is also there between silicate cations (ΣCat_s) and $^{87}Sr/^{86}Sr$ (Fig 4.30) further supporting this contention.

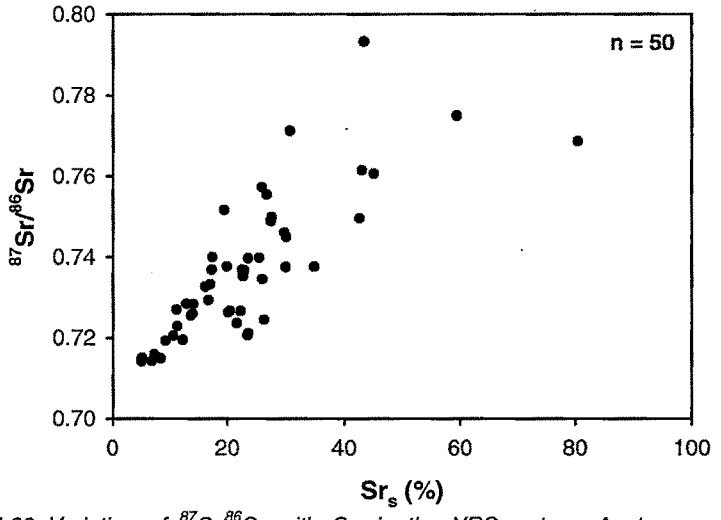

Fig. 4.29 Variation of $^{87}Sr/^{86}Sr$ with Sr_s in the YRS waters. A strong positive correlation (r^2 = 0.64) is suggestive of the dominance of silicate weathering in regulating the Sr isotopic composition of the YRS rivers.

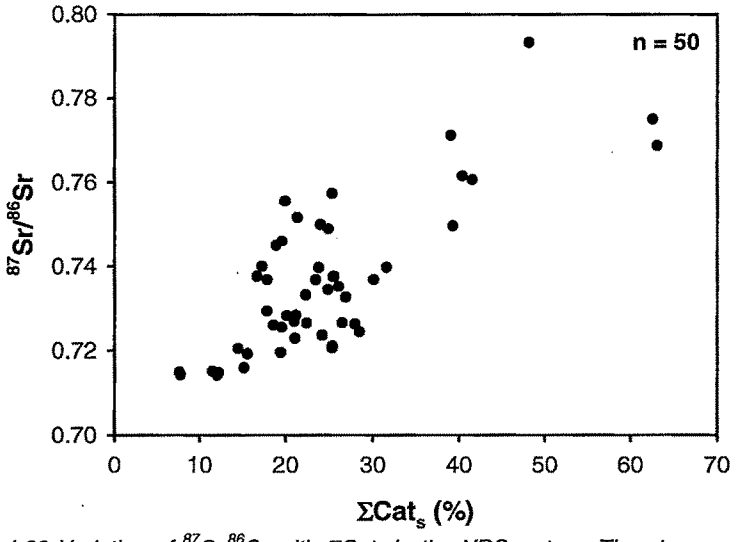

Fig. 4.30 Variation of $^{87}Sr/^{86}Sr$ with ΣCat_s in the YRS waters. The strong positive correlation (r^2 = 0.61) suggests that silicate weathering exerts a dominant role on the radiogenic Sr isotopic composition of rivers.

The contribution of Sr from carbonate weathering can be calculated as:

$$Sr_c\ (nM) = (Ca_r - Ca_s) \times [Sr/Ca]_c$$

$(Sr/Ca)_c$ has been taken to be the abundance ratio in LH Precambrian carbonate outcrops, 0.20±0.15 nmol/μmol (Singh et al., 1998). This calculation assumes that all Ca in the rivers come from only two sources, silicates and carbonates, that Sr and Ca are released from carbonates in the same proportion as their abundances and behave conservatively after their release to rivers. Sr_c thus calculated has a range of 3 to 37% with an average of 14±7%. In the Yamuna sampled at Batamandi, Sr_c varies between 9 to 11% for the three different seasons and at Hanuman Chatti, Sr_c varies between 20-27%, quite similar to Sr_s. In the spring waters of Kempti Fall and Shahashradhara Sr_c is only 3-4%. Considering that easily weatherable rocks like evaporites and phosphates occurring in the Yamuna catchment also contribute to the Ca in the rivers, this estimate of Sr_c calculated as above would be a *maximum*. In most of the streams Sr_s and Sr_c do not add up to 100% though in a few of them the Sr balance can be achieved within the errors of estimation. This suggests that there are sources in addition to silicates and Precambrian carbonates for Sr in these rivers. From the knowledge on the lithology of the Yamuna basin, the additional sources contributing Sr to these rivers are evaporites, phosphates and/or carbonates other than the Precambrian carbonates studied by Singh et al. (1998). Assuming that *all* SO_4 in the YRS rivers are of evaporite origin (with equivalent amount of Ca), and using an average Sr/Ca ratio, 2.9 (nM μM^{-1}) for evaporites (Wedepohl, 1978), an *upper limit* of their contribution to the Sr budget can be estimated. The estimates show that, in a few of the streams, all Sr can be of evaporite origin.

An approach to resolve the contributions of various sources to the Sr budget in the waters is to plot $^{87}Sr/^{86}Sr$ vs. Ca/Sr (Blum et al., 1998; Fig. 4.24). The data points fall in the mixing space defined by evaporites, silicates and carbonates. The high $^{87}Sr/^{86}Sr$ in the YRS is a result of silicate Sr end member. It is seen that many of the data points fall close to the end member compositions of evaporites and phosphates (with Ca/Sr ~0.2-0.5 μM/nM, and $^{87}Sr/^{86}Sr$ ~0.71) underlining their importance in contributing to the Sr budgets of the YRS. The average composition of the Precambrian outcrops plot far off the river water data suggesting that their influence on the Sr load in the river waters is not quite significant consistent with the estimation of Sr_c (average ~15% for the YRS).

The results of Sr mass balance in a few selected YRS streams are given in Table 4.9. The calculations for $^{87}Sr/^{86}Sr$ were done using a value of 0.8 for silicate end member $^{87}Sr/^{86}Sr$ (Krishnaswami et al. 1999) and 0.71 for carbonates and evaporites. It is seen that for the streams which have comparable areal distribution of various lithologies (e.g. RW98-4, RW98-8, RW98-13, RW98-32, RW98-33), the calculated and the measured $^{87}Sr/^{86}Sr$ values agree reasonably. All these rivers have $^{87}Sr/^{86}Sr \leq 0.74$. In contrast, for rivers flowing mainly through crystallines (RW98-16, RW98-18, RW98-26, RW98-27) and which have $^{87}Sr/^{86}Sr > 0.75$, the calculated values are significantly lower than the measured ones. Even if a higher value of 0.83 (obtained for 100% $(\Sigma Cat)_s$ end member, Fig. 4.30) is used for silicate end member, the calculated $^{87}Sr/^{86}Sr$, though agrees better, still remains lower than the measured values. One likely explanation for this discrepancy is that ^{87}Sr may be preferentially released to these rivers from minerals such as biotite which generally have higher $^{87}Sr/^{86}Sr$ than the whole rock values used in the calculation. The recent experimental studies on biotite weathering show that ^{87}Sr, indeed, is preferentially released from them to the weathering solution (Taylor et al., 2000a).

Table 4.9 Sr mass balance in selected YRS streams.

Sample/River	Sr_s (%)	Sr_c (%)	Sr_{rest} (%)	$^{87}Sr/^{86}Sr_{cal}$	$^{87}Sr/^{86}Sr_{meas}$
RW98-16/Yamuna@Hanuman Chatti	20	19	61	0.7276	0.7516
RW98-18/Didar Gad	43	11	45	0.7490	0.7932
RW98-26/Godu Gad	59	6	34	0.7635	0.7749
RW98-27/Tons@Mori	45	15	40	0.7506	0.7606
RW98-4/Yamuna@Rampur Mandi	22	10	69	0.7295	0.7236
RW98-8/Aglar	5	5	90	0.7147	0.7150
RW98-13/Barni Gad	30	22	48	0.7370	0.7375
RW98-32/Tons@confluence	11	7	82	0.7201	0.7269
RW98-33/Yamuna@Saharanpur	21	11	69	0.7284	0.7266

Calculations were done using $^{87}Sr/^{86}Sr$ for silicate end member as 0.8 and 0.71 for carbonates and the rest (evaporites and phosphates) end members. It was assumed that $Sr_s+Sr_c+Sr_{rest} = 100\%$. Sr_s is estimated using value of $(Sr/Na)_{sol} = 2.0$. Sr_c is the lower limit, estimated assuming all SO_4 are of evaporite origin. Values of Sr_s, Sr_c and Sr_{rest} given have been rounded off, whereas $^{87}Sr/^{86}Sr$ were calculated using the actual values.

More recently, calcites occurring as veins in granites and granodiorites in the Himalaya have been proposed a source for the high radiogenic $^{87}Sr/^{86}Sr$ to the rivers draining these basins (Blum et al., 1998; Jacobson and Blum, 2000). The carbonate content of these

rocks from the Nanga Parbat massif in north Pakistan and Raikhot watershed coupled with their highly radiogenic Sr isotope composition (~0.9, quite similar to those in the host silicates) led to this proposition. The role of vein-calcites in the budget of Sr and its isotopes in the YRS is discussed below.

The carbonate contents in four granite samples from the Yamuna catchment collected around Hanuman Chatti range from ~0.2 to 0.9% with an average 0.6% (Table 4.2), similar to calcite contents in silicates of Nanga Parbat massif (Jacobson and Blum, 2000). The Sr/Ca in calcites from Nanga Parbat, determined by mild acid leach, is ~0.45 (nM/μM). Assuming that (i) the average carbonate content of the YRS crystallines is 0.6% with Sr/Ca of 0.45 nM/μM, (ii) the suspended matter concentration of the YRS is ~2 g $\ell^{-1}$and (iii) *all Ca and Sr* are released to waters from these calcites during weathering, it can be estimated that the contribution from the vein-calcites to the Sr budget of the YRS would be, on an average, about 10%. This estimate would go up by a factor of two, if bed load is also considered such that the total erosion is twice the suspended matter concentration (Galy and France-Lanord, 2001). Such an estimate, however, is not valid for rivers such as the Didar Gad, as the calculated Ca from vein-calcites exceeds the measured Ca concentration in them. Therefore, an *upper estimate* of Sr contribution from vein-calcites for such streams can be made assuming that *all Ca* in them is of vein-calcite origin. Such a calculation shows that in Didar Gad and Godu Gad, vein-calcites can contribute a maximum of ~33-40% and ~23-30% respectively of their total Sr, compared with their estimated silicate contributions of 43% and 59% respectively. These are *upper limits* of vein-calcite contributions, as part of Ca has to be from silicates and other sedimentaries. If all the non-silicate Ca is assumed to be of vein-calcite origin, then vein-calcite contribution to their Sr load would be ~26% and ~14% respectively. These calculations show that in the YRS streams flowing through crystallines, vein calcites can be an important contributor to their Sr budget, the magnitude of their contributions, however, awaits better determination of their abundance and their Sr content. Their role in influencing the high $^{87}Sr/^{86}Sr$ in the YRS needs to be evaluated by careful sampling and analysis of Sr, Ca and $^{87}Sr/^{86}Sr$ in them. In this study, co-variation of $^{87}Sr/^{86}Sr$ with SiO_2/TDS, $(Na^*+K)/TZ^+$, Sr_s and $(\Sigma Cat)_s$ favour the hypothesis that silicate weathering dominate the high radiogenic Sr isotopic composition of the YRS.

Laboratory experiments (Taylor et al., 2000a) on phlogopite and biotite containing trace calcites in them, show that at steady state, the rate of calcite dissolution is either similar to that of phlogopite or 50% slower than the biotite dissolution. In the initial phase of their experiments, release of Sr from trace calcites in phlogopites and biotites were about 3 and 2 times faster respectively than that at steady state. At steady state, the dissolution rate of trace calcites was limited by the rate of their exposure to the weathering solution, which in turn is controlled by the rate of silicate dissolution. In another laboratory experiment on rate of Sr release from labradorites and trace calcites in them (Taylor et al., 2000b), it was observed that in the first samples of output solutions in each experiment, even with faster Sr release from calcites, only ~1% of Sr was derived from their dissolution. The calcite contribution to Sr in these solutions decreased rapidly with time and at steady state, it became negligible. $^{87}Sr/^{86}Sr$ of the output solutions further indicated that calcite solution had minimal effect on Sr release rates, as none of the output solutions had $^{87}Sr/^{86}Sr$ significantly less than the plagioclase ($^{87}Sr/^{86}Sr$ of the calcite, based on acetic acid leach, was less than that of plagioclase). In the Himalaya, with high physical erosion, exposure of fresh calcites may not be a limiting factor for vein-calcite dissolution, however, considering that the abundance of vein calcites in the YRS basin is ~0.6% with Sr/Ca ~0.45, for them to be of comparable significance as silicates in Sr budgets of the rivers, they need to release Sr at a rate at least 10^3 times faster than silicates. Such a requirement is not likely to be met in the light of experimental studies (Taylor et al., 2001a, b) which show that at any stage of weathering, release of Sr from trace calcites can, at the most, be three times as fast as that from silicates. Hence though the upper estimates of Sr contributions of vein-calcites show that they can be significant in the YRS Sr budget, a proper assessment of their impact remains unresolved and needs better sampling and analysis of vein calcites for $^{87}Sr/^{86}Sr$, Sr and Ca. Available measurements are based on mild acid leaching (Jacobson and Blum, 2000), more careful analysis are needed to avoid silicate interference. Further, the origin of these vein calcites needs to be better understood. If these calcites formed as an intermediate step in the weathering of silicates then, at steady state, their contribution to Sr budget and $^{87}Sr/^{86}Sr$ can be considered as that arising from silicates themselves.

4.2.5 Dissolved Barium in the YRS

Ba abundances in the YRS range from ~17 to 870 nM (Table 4.1). Its abundance, in general, is lower (<100 nM) in the Yamuna and its tributaries in their upper reaches, a trend similar to that observed for major ions and Sr. The streams in the upper reaches draining predominantly crystallines have lower Ba, the Didar Gad has the lowest (17 nM, Table 4.1). In the lower reaches Ba concentrations are higher in the Yamuna mainstream as well as its tributaries and show large variation. The Asan river originating from the Mussoorie ridges and its tributary *Tons* at Dehradun have very high Ba (~760 and ~530 nM respectively in post-monsoon samples). Ba concentrations in the YRS rivers in the upper reaches are similar to those in the Trisuli draining the Higher Himalayan Crystallines in the Nepal Himalaya (Chabaux et al., 2001) whereas Ba in the lower reaches of the YRS are higher and similar to those observed in the Narayani and Kali rivers in the Nepal Himalaya (Chabaux et al., 2001). Ba abundances in the YRS water show significant positive correlation with Ca and Sr (Fig. 4.31), indicating that they may have a common source such as minerals rich in Ca; carbonates, evaporites and phosphates.

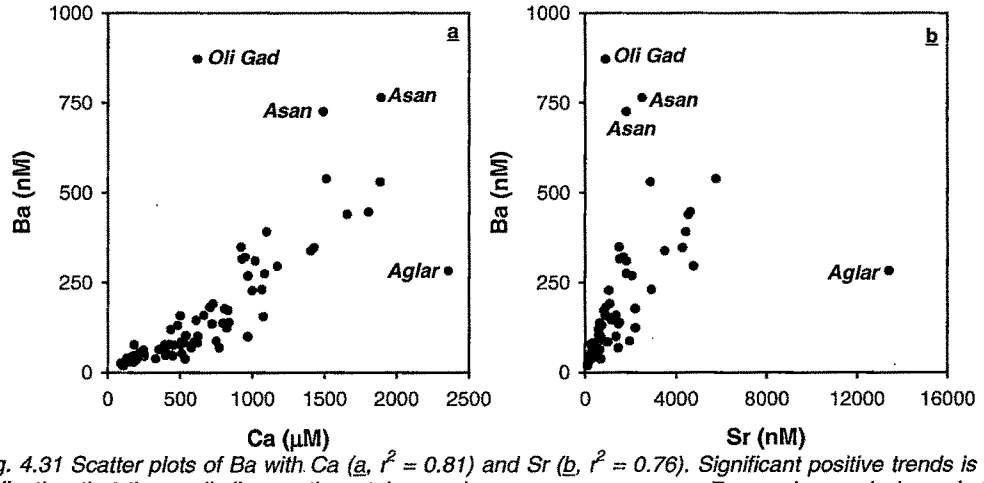

Fig. 4.31 Scatter plots of Ba with Ca (a, r^2 = 0.81) and Sr (b, r^2 = 0.76). Significant positive trends is an indication that these alkaline earth metals may have common sources. Regression analysis excludes four samples marked in the plots.

The relative importance of these lithologies in contributing to dissolved Ba in the YRS waters would be discussed in later sections. The stream Oli Gad with the highest Ba (870 nM) fall far away from the general trend (Fig. 4.31). The other two rivers that fall off the trend set by the other samples are the Asan and the Aglar. The river Asan originates from

around Mussoorie Ridge where phosphorites are known to occur containing high Ba concentrations (Mazumdar, 1996). A significant part of the Aglar drainage basin is in Krol carbonates, which are known to have pockets of gypsum in them. High Ca and Sr in the Aglar waters most likely are derived from gypsum dissolution.

Dissolved Ba shows co-variation with Ca, Mg, Na* and SO_4 (Figs. 4.31, 4.32), similar to Sr, suggesting that it is also derived from multiple sources such as silicates, carbonates, evaporites and phosphates. Ba/Ca (nM/μM) in the YRS waters range from 0.07

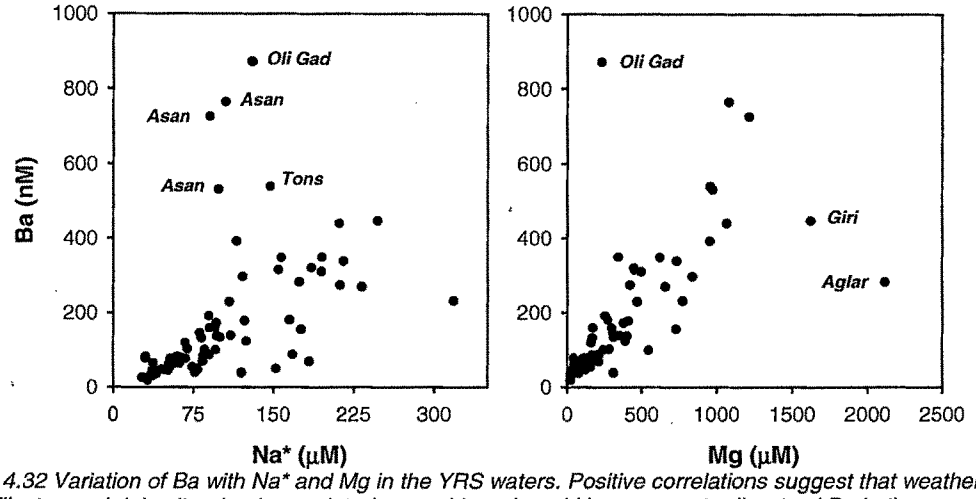

Fig. 4.32 Variation of Ba with Na and Mg in the YRS waters. Positive correlations suggest that weathering of silicates and dolomites (and associated assemblages) could be sources to dissolved Ba in these waters (see text).*

to 1.4 with a mean, 0.23. In order to assess if Ba/Ca in the YRS waters are changed via precipitation of barite, barite saturation index was calculated at 25 °C using Ba and SO_4 concentration data. It was found that all the water samples analyzed in this study are undersaturated with barite, which argues against any removal of Ba from the waters by $BaSO_4$ precipitation. It has already been discussed earlier that in the present study there is no evidence of calcite precipitation in the YRS waters. Ba abundance in the Krol carbonates are lower than those in the crystallines (Mazumdar, 1996), with Ba/Ca 0.03-0.11 nM μM^{-1} (mean: 0.06±0.03 nM μM^{-1}). Analogous to Sr, dissolved Ba/Ca in these waters are significantly higher than those in carbonates. This would indicate that these carbonates are not an important source of Ba to these waters on a basin wide scale. If average Ba/Ca in the Krol carbonates (0.06) is taken to be representative of all carbonates in the YRS basin, carbonate contributions to dissolved Ba in the YRS waters can be estimated under the

assumptions that (i) Ba and Ca are released to waters in the same proportion as their abundance in the carbonates, (ii) *all* Ca in the YRS waters are derived from carbonates and (iii) both Ba and Ca behave conservatively after their introduction to the rivers. The calculations show that carbonates can contribute ~4 to 85% of the dissolved Ba in the YRS waters (mean: 32±14%). Considering that Ca in these waters is also derived from silicates, evaporites and/or phosphates, these estimates are *upper limits*.

Crystallines and sedimentary silicates, which are dispersed throughout the drainage basin, can be another source for Ba. We can estimate silicate contributions to the dissolved Ba in the YRS waters using Na* as and index of silicate weathering. The difficulty in such estimation is proper assessment of the ratio Ba/Na, which is released from silicates to waters. The similar ionic radii of Ba and K allow Ba to replace K in crystal lattice of minerals in igneous rocks. This would make the release of Ba from crystallines difficult as K-bearing minerals are more resistant to chemical weathering. Further, during weathering of crystallines, Ba is likely to be retained in clay fractions and Fe-oxyhydroxides. Ba shows significant positive correlation with K and Al in the YRS bed sediments (Fig. 4.33). The outlier in these plots is the sample from the river Aglar, which drains a significant part of Krol carbonates and has as high as ~44% carbonate in its sediment. Co-variation of Ba with K and Al, together with the observation that Ba concentrations in the carbonate-free bed sediments, in general, are either similar or higher than those in the granites analyzed in this study (Table 4.2), is an indication that during silicate weathering Ba tends to remain in the clay fractions or Ba occurs in minerals more resistant to weathering, hence its release to waters may be minimal. Ba/Na in granitic bed rocks in the Yamuna basin is lower than those in the carbonate free bed sediments, suggesting that Na is preferentially released to waters from rocks relative to Ba which is either released slower or retained in the residual clay fractions. Hence Ba/Na in rivers would be lower than those in silicates. Godu Gad, a stream flowing predominantly through silicates, has the lowest Sr/Na* and Ba/Na* (~0.3 nM μM^{-1}), high $^{87}Sr/^{86}Sr$ (0.7750) and the highest proportion of silicate cations $(\Sigma Cat)_s$. Using this value (0.3) as the Ba/Na ratio released to waters from silicates, it can be estimated that silicates can contribute ~4 to 95% of the dissolved Ba in the YRS (mean: 27±18%). They can account for bulk of Ba in the streams with low Ba abundances, <70 nM. The observation that the streams Didar Gad and Godu Gad, draining predominantly silicates, have very low Ba, 17 and ~45

nM suggests that rivers with higher Ba concentrations have to derive their Ba from sources enriched in Ba. Ba abundances in the YRS show an inverse correlation with silicate cations $(\Sigma Cat)_s$ further supporting the idea that contribution from silicates can not account for the measured higher Ba concentrations in many of the rivers.

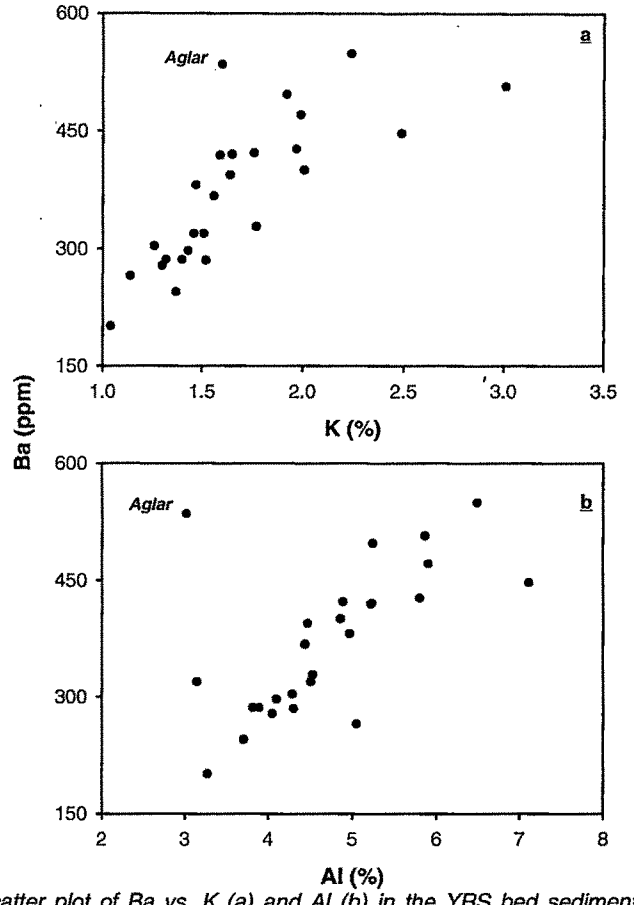

Fig. 4.33 Scatter plot of Ba vs. K (a) and Al (b) in the YRS bed sediments. Ba shows positive correlation with K (r^2=0.69) and Al (r^2=0.68), suggestive of more resistant host minerals of Ba and/or possible retention of Ba in the clay fractions during chemical weathering. Regression analysis excludes the sample from Aglar (RS98-8, see text)

A plot of $^{87}Sr/^{86}Sr$ vs. 1/Ba in the YRS waters shows that samples by and large fall on a two component mixing line (Fig. 4.34). The high $^{87}Sr/^{86}Sr$ and low Ba end member is defined by silicates, consistent with earlier estimates that for streams with low Ba abundances, silicates can be a major contributor. The intercept of the regression line in Fig. 4.34 is 0.716, similar to the $^{87}Sr/^{86}Sr$ of Pc carbonates of the YRS basin and phosphates analyzed in this study but marginally higher than that for evaporites, suggesting that for

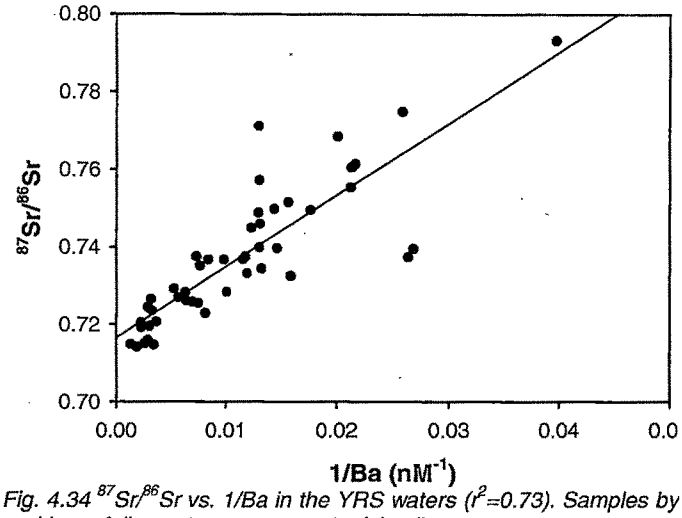

Fig. 4.34 $^{87}Sr/^{86}Sr$ vs. 1/Ba in the YRS waters (r^2=0.73). Samples by and large fall on a two component mixing line.

streams with higher Ba abundances, phosphates, carbonates and evaporites could be dominantly contributing to their Ba. The observation that spring waters of Shahashradhara has only ~80 nM Ba, suggests that evaporite contribution can not possibly account for high abundances of Ba in many of the YRS streams. Phosphorites from Maldeota and Deomala mines have been reported to have high Sr and Ba concentrations (Mazumdar, 1996). The river Asan and its tributary *Tons*, draining the area around Mussoorie, a region where phosphorites are known to occur in the Tal Formation, have very high Sr and the highest Ba concentrations among all the YRS streams analyzed. This spatial correlation is an indication that phosphorites may be a dominant source of Ba in rivers flowing thorough them.

Analogous to Sr, Ba correlates well with dissolved Re in the YRS, with more scatter at higher Ba concentrations (Fig. 4.35). As already discussed, Re is mainly derived from organic rich sediments, the sulphuric acid released via oxidation of pyrites associated with the organic sediments weather other lithologies which occur along with them, such as phosphorites and carbonates. This underlines the importance of H_2SO_4 weathering of phases such as phosphates in releasing these trace elements to the river waters. The outliers in the Re-Ba plot, the river Asan and its tributary *Tons*, draining phosphates and Krol carbonates (and possibly evaporites), may have derived high Ba from them with little contributions of Re. Barites are known to occur as pockets and veins in Krol limestones (Anantaraman and

Bahukhandi, 1984), however, considering that barites are relatively insoluble it is uncertain if they can dissolve and contribute significantly to dissolved Ba in these rivers.

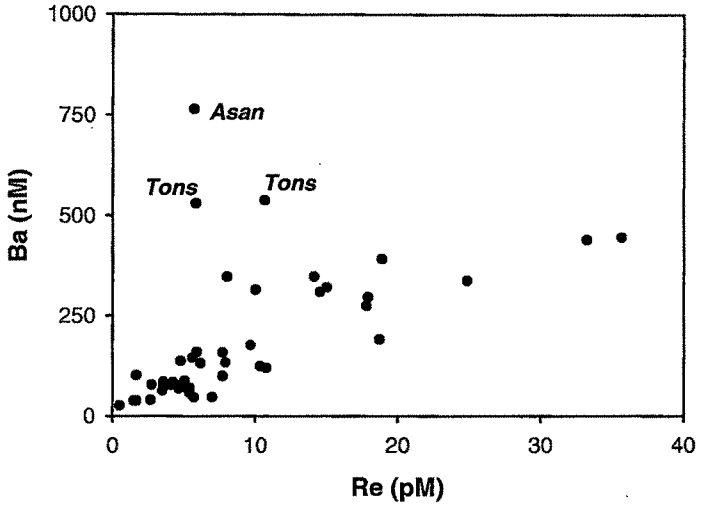

Fig. 4.35 Scatter plot of Ba vs. dissolved Re in the YRS waters. Both these dissolved properties co-vary, with more scatter at higher Ba concentrations. This trend suggests that release of Re to these waters is accompanied by proportionate release of Ba from lithologies associated with organic rich sediments such as phosphates and carbonates.

4.2.6 Weathering rates and CO_2 consumption

The data on silicate and carbonate components of cations in rivers, its silica concentration, coupled with information on the drainage area and discharge can be used to calculate the present day silicate and carbonate weathering rates in their basins. For the Yamuna, the discharge data is available at Tajewala, which is a few tens of kms downstream of Batamandi. For calculation of silicate weathering rate (SWR), the silicate cation contributions (K_s, Na_s, Ca_s and Mg_s) and silica abundances (all in mg ℓ^{-1}) are summed up and for carbonate weathering rate (CWR), Ca and Mg from carbonates and stoichiometric equivalent of carbonate were added up. Such calculations show that SWR in the YRS in the Himalaya is ~11 mm ky^{-1} which is ~4 times lower than the CWR, ~43 mm ky^{-1}. The SWR and CWR becomes ~10 and ~46 mm ky^{-1} respectively if $(Ca/Na)_{sol}$ is decreased from 0.7 to 0.35. The CWR has been estimated assuming all non-silicate Ca and Mg to be of carbonate origin. Considering that evaporites also contribute to Ca in the rivers, such an estimate of

CWR would be an *upper limit*. Assuming that all SO_4 in the river to be of evaporite origin, a *lower limit* of CWR is estimated to be ~31 mm ky^{-1}. Using a suspended load of 2 g ℓ^{-1} in the YRS (Subramanian and Dalavi, 1978; Hay, 1998), mechanical erosion in the basin is estimated to be ~2.3×10^3 tons km^{-2} y^{-1}, about 15 times higher than the total chemical erosion (silicate and carbonate weathering) rates in the basin. This underlines the importance of mechanical erosion in an active mountain chain such as the Himalaya.

The flux of CO_2 consumed during silicate weathering (ϕCO_2 in moles km^{-2} y^{-1}) in the Yamuna basin has been estimated from the calculated silicate cations, river discharge and the basin area: $(\phi CO_2) = \phi\ (TZ^+)_{sil}$. This estimation gives a value of (ϕCO_2) ~7×10^5 moles km^{-2} y^{-1} at Batamandi. This would become ~6×10^5 moles km^{-2} y^{-1} if a value of 0.35 is used for $(Ca/Na)_{sol}$ instead of 0.7. These estimates based on the major ion composition of the monsoon sample (RW99-55) would be upper limits considering that the sulphuric acid, as already discussed, also provide protons for chemical weathering in the YRS basin. If it is assumed that all SO_4 in the waters result from pyrite oxidation, the lower limit of CO_2 consumption would be is ~$(5\text{-}6)\times10^5$ moles km^{-2} y^{-1}. In making these calculations the protons provided by H_2SO_4 and H_2CO_3 are assumed to be in the same ratio (equivalence) as the SO_4/HCO_3 abundance in the water. Independent estimates of (ϕCO_2) can be made from the Si abundances in the waters: $(\phi CO_2) = 2\phi Si$, this relationship is derived for aluminosilicate weathering in general, based on the global fluvial dataset (Huh et al., 1998 and references therein). Such an approach gives an estimate of ~4×10^5 moles km^{-2} y^{-1}. Thus, CO_2 consumption flux via silicate weathering in the YRS estimated by various approaches is ~$(4\text{-}7)\times10^5$ moles km^{-2} y^{-1}.

4.2.7 Comparison of silicate weathering CO_2 consumption rates with other river basins

Comparison of results of weathering rates estimated in this study with those available for the headwaters of the Ganga, in the Alaknanda and Bhagirathi basins (Krishnaswami et al., 1999) suggest that SWR is ~2 times and CWR ~2-3 times higher in the YRS (Table 4.10). The CO_2 consumption flux for silicate weathering, in the Yamuna basin in the Himalaya calculated using various approaches vary between $(4\text{-}7)\times10^5$ moles km^{-2} y^{-1}. Krishnaswami et al. (1999) reported a value of ~4×10^5 moles km^{-2} y^{-1} for the Bhagirathi and Alaknanda basins in the Himalaya. This is about a factor of two lower than that in the YRS

basin, calculated following the same approach, assumptions and end member values. The CO_2 consumption flux calculated in this study for the Ganga at Rishikesh varies between 2-3×10^5 moles km^{-2} y^{-1} (Table 4.10), compared to ~4×10^5 moles km^{-2} y^{-1} reported by Krishnaswami et al. (1999). This difference arises from the variability in the major ion composition of river water samples used for calculations. In this study, calculations for the Ganga were done using the major ion concentrations of the monsoon sample (RW99-59) whereas Krishnaswami et al. (1999) used those for the sample of April collection. This underlines the importance of using discharge weighted concentrations for such calculations to have more reliable estimates of the CO_2 drawdown via silicate weathering. However, considering that about 80% of the water flow of the YRS occurs during monsoon season, estimates based on the cation concentrations during this period (an approach adopted in this work) is more representative of the whole year. The CO_2 consumption fluxes in these rivers basins in the Himalaya compare with values of ~0.5×10^5 moles km^{-2} y^{-1} in the Amazon, ~0.5×10^5 moles km^{-2} y^{-1} in the Congo-Zaire (Gaillardet et al., 1995; 1997;1999) and ~1.5×10^5 moles km^{-2} y^{-1} in the Orinoco (Edmond and Huh, 1997). The CO_2 consumption fluxes in the Ganga-Yamuna basins in the Himalaya are higher than those in the river basins of the Huanghe (~0.82×10^5 moles km^{-2} y^{-1}), the Xijiang (~0.55×10^5 moles km^{-2} y^{-1}), the Changjiang (~0.59×10^5 moles km^{-2} y^{-1}), in the northern slopes of the Himalaya (Gaillardet et al., 1999). In the Mekong basin it is ~2.4×10^5 moles km^{-2} y^{-1}, comparable to that in the Ganga basin but marginally lower than that in the Yamun basin.

Table 4.10 Weathering rates and CO_2 consumption in the river basins in the Himalaya[a)]

River basin	Location	Discharge 10^{12} ℓ y^{-1}	Area 10^3 km^2	SWR (i)	SWR (ii)	CWR (i)	CWR (ii)	CO_2 drawdown[b)]
Yamuna	Batamandi	10.8	9.6	25-28	~10	115-123	43-46	4-7
Bhagirathi[c)]	Devprayag	8.3	7.8	15.2	5.8	41.1	15.2	4.1
Alaknanda[c)]	Bhagwan	14.1	11.8	10.2	3.9	63.2	23.4	3.6
Ganga	Rishikesh	22.4	19.6	12-13	~5	54-56	20-21	2-3
Ganga[c)]	Rishikesh	22.4	19.6	12.9	4.9	51.7	19.1	3.8
Narayani[d)]	Narayangha	49.4	31.8		7.0		52.0	
G-B[c)]		1002	1555	13.6	5.3	31.7	11.7	3.3

Yamuna and Ganga estimates based on monsoon samples (RW99-55 and RW99-59). [a)]calculated using the mean density 2.6 and 2.7 g cm^{-3} for silicates and carbonates respectively; (i): tons km^{-2} y^{-1}; (ii): mm ky^{-1}. [b)]drawdown via silicate weathering in 10^5 moles km^{-2} y^{-1}. [c)]from Krishnaswami et al. (1999). [d)]from Galy and France-Lanord (1999).

From such comparisons, it is borne out that the present day CO_2 consumption rates in the river basins in the southern slopes of the Himalaya are significantly higher than those from other major global river basins in the world. These estimates indicate that the contemporary CO_2 drawdown by silicate weathering in the Yamuna and the Ganga basin in the Himalaya is disproportionately higher than other global rivers. Enhanced silicate weathering resulting from conducive climate, relief and environmental factors could be responsible for this (Raymo and Ruddiman, 1992). However, the impact of this on the global CO_2 consumption by silicate weathering is not that pronounced as the G-B basin account for only ~1.5% of the global drainage area and contribute only ~4% of the global CO_2 drawdown. The upper reaches of the Ganga and the Yamuna are dominated by physical erosion with less intense chemical weathering.

4.2.8 Chemical weathering: control of temperature and altitude

Earlier studies have shown that chemical weathering in river basins depends on several factors such as lithology, elevation, temperature and runoff (Drever and Zobrist, 1992; White and Blum, 1995). In many of the river systems the variation in solute fluxes with temperature, r_T, has been described in terms of the Arrhenius relation:

$$r_T = Ae^{(-E_a/RT)}$$

where E_a is the activation energy (kJ mol^{-1}), T the temperature (K), R the gas constant and A the pre-exponential constant. A plot of ln r_T (or solute concentration) against 1/T would yield a straight line with a slope of ($-E_a/R$) from which the activation energy can be calculated. This relation, though is oversimplified to be applied to solute fluxes in natural watersheds in which chemical weathering reactions are dependent on multiple variables, has been used to empirically determine the activation energy for weathering of various lithologies (White and Blum, 1995; Dessert et al., 2001).

The use of such an approximation for studying granite weathering has been a topic of debate. Jenny (1941), based on study of large number of soils in the United States, had observed, in case of granite-gneiss weathering, an increase of clay content with temperature that is greater for higher precipitation. Berner and Berner (1997) observed that higher global temperature and greater rainfall should enhance silicate weathering. On the contrary,

Edmond and Huh (1997) and Huh and Edmond (1999), based on studies of Siberian rivers and other river basins in the tropical regions, concluded that lithology and their exposure to weathering plays the dominant role in regulating solute fluxes and weathering rates, the role of climate being secondary. In Fig. 4.36, the log concentrations of Na* and Si (proxies of silicate weathering) are plotted against (1/Temp.) in samples of selected rivers and streams of the YRS for the summer collection. (only data for tributaries are plotted to minimize averaging effects.

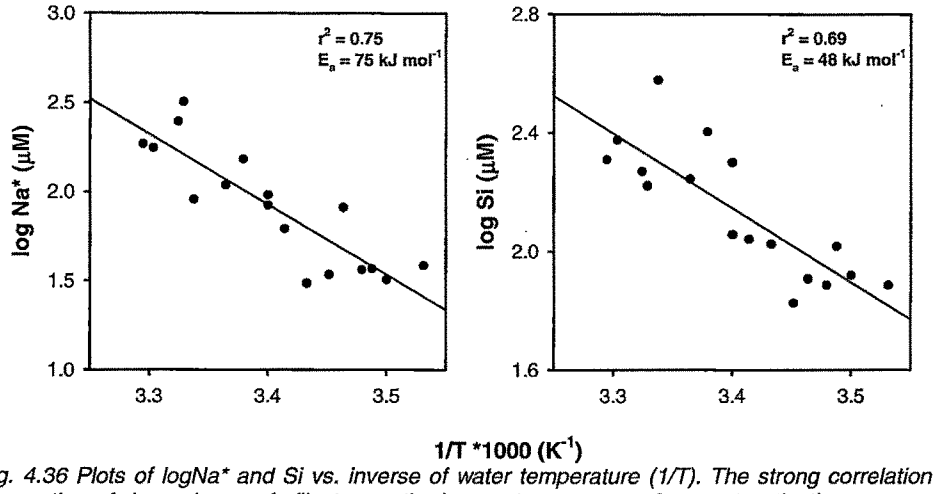

Fig. 4.36 Plots of logNa and Si vs. inverse of water temperature (1/T). The strong correlation is suggestive of dependence of silicate weathering on temperature. Apparent activation energy for overall silicate weathering in the basin has been calculated from the slopes of the regression lines to be 75 and 48 kJ mol^{-1}.*

The data of the Yamuna and Tons mainstreams are not included in the plot as they integrate the chemistry along their path). October samples could not be plotted, as temperature measurements were not made during this campaign. Similarly, the monsoon samples had marginal temperature spread, 15.7 to 27.4 °C, as sampling was restricted to lower reaches of the YRS. The plots show a significant anticorrelation of log concentration with inverse of temperature (r^2 = 0.75 for Na*, and 0.69 for Si). Such a trend is consistent with that expected based on Arrhenius relation. From the slope of the regression lines, the "apparent activation energy" for silicate weathering in the YRS basin is derived to be ~75 and ~48 kJ mol^{-1}.

In natural systems like the YRS basin, in addition to temperature, other factors such as altitude, rainfall and vegetation also influence the silicate weathering in the basin and hence the solute concentrations in the river waters. Indeed, the data show significant negative

correlation between logNa*(Si) and sampling altitude (Fig. 4.37). This may be a manifestation of temperature which decreases with altitude. In Chapter 3, the interdependence of $\delta^{18}O$ (a proxy for altitude) and ΣCat^* has been used to assess the variation in weathering contribution (in terms of ΣCat^*) in the Yamuna waters with altitude (Dalai et al., 2001d).

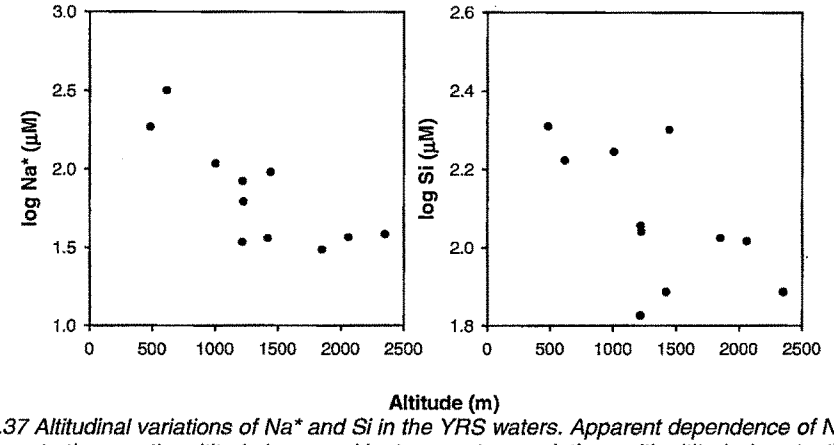

Fig. 4.37 Altitudinal variations of Na and Si in the YRS waters. Apparent dependence of Na* and Si concentrations on the altitude is caused by temperature variations with altitude (see text).*

The deduced values of activation energy are average for the silicates (crystallines and metasediments) as a whole in the YRS basin. These values are similar to those obtained for granitoid weathering in natural watersheds, 77 kJ mol^{-1} (Velbel, 1993), 69-78 kJ mol^{-1} (White and Blum, 1995) and 51 kJ mol^{-1} (White et al., 1999) and those determined from laboratory weathering studies, 56-61 kJ mol^{-1} for granitoid rocks (White et al., 1999), 60 kJ mol^{-1} for albite and 80 kJ mol^{-1} for oligoclase (White and Blum, 1995 and references therein). The strong negative correlation between logNa*(Si) and 1/T and the similarity between the activation energy estimated in natural watersheds and that measured in the laboratory experiments reinforces the idea that climatic parameters like temperature influences chemical weathering of silicates, though this dependence could manifest through other factors such as altitude, rainfall and vegetation.

4.3 CONCLUSIONS

The headwaters of the Yamuna and its tributaries in the Himalaya have been extensively sampled for three different seasons. The major ion, Sr and Ba abundances and $^{87}Sr/^{86}Sr$ in the river waters, sediments and bedrocks have brought out the following important observations and conclusions.

1. The YRS waters are mildly alkaline, with a wide range of TDS, ~32 to ~620 mg ℓ^{-1}. The streams in the lower reaches have higher TDS than those near the source region. This is caused by a number of factors, such as, the abundance of more easily weatherable rocks (carbonates and evaporites) in the lower reaches; higher temperature and vegetation. The Sr and its isotopic composition in the YRS is dictated by the lithology. $^{87}Sr/^{86}Sr$ in the Yamuna decreases downstream with a rise in Sr.
2. Ca and alkalinity are the most abundant among the major ions in the YRS waters, indicating the dominance of carbonate weathering in contributing to their dissolved loads. However, their contribution to the dissolved Sr and Ba in the YRS is comparatively lower (~15% and ~30% respectively). With lower Sr/Ca and $^{87}Sr/^{86}Sr$ than the river waters, carbonates are not a major contributor to the high $^{87}Sr/^{86}Sr$ of river waters. Bulk of the water samples is supersaturated with calcite. Furthermore, decrease of Ca/Mg in the waters with an increasing Ca suggest that either dolomite weathering or precipitation of calcites may result in such a trend. In the present study, however, no evidence of calcite precipitation was observed.
3. Silicates, on an average, contribute ~25% (on a molar basis) to the total cations in the YRS waters the rest coming from carbonates, evaporites and phosphates. Maximum contribution of cations from carbonates and evaporites in the YRS basin are ~74 and ~21%. The contributions of silicates to the YRS cation budget is similar to their contribution to the dissolved Sr (~25%) and Ba (~30%). Disseminated calcites though may contribute significantly to the dissolved Sr in the YRS, their role in regulating the $^{87}Sr/^{86}Sr$ of the rivers needs to be assessed by carrying out more detailed work. The present data set clearly show that silicate weathering dominates the high $^{87}Sr/^{86}Sr$ of the YRS, as evident from the correlation of $^{87}Sr/^{86}Sr$ with SiO_2/TDS, $(Na^*+K)/TZ^+$, Sr_s and $(\Sigma Cat)_s$. Minor lithologies such as evaporites and phosphates seem to be significant

contributors to the YRS Sr and Ba budgets and they play a diluting role in $^{87}Sr/^{86}Sr$ of these rivers.

4. The silicate weathering rate in the Yamuna basin is ~10 mm ky^{-1}, 3 to 4 times lower than the carbonate weathering rate, ~31-46 mm ky^{-1}. Chemical weathering of silicates in the Yamuna basin in the Himalaya, however, is not intense, as evident from the low values of Si/(Na*+K) in the waters (~1.2) and low values of CIA (~60) in the bed sediments. The CO_2 drawdown via silicate weathering in the YRS and the Ganga basins in the Himalaya are similar and a few times higher than those reported in the other major river basins of the world. The impact of such enhanced drawdown in the southern slopes of the Himalaya on the global CO_2 budget is not pronounced as the drainage area and discharge of the Yamuna and the Ganga in the Himalaya constitute only a low proportion of the global values.
5. The strong correlation of logNa*(Si) vs. 1/T implies the dependence of silicate weathering on temperature. Apparent activation energy calculated for overall silicate weathering in the basin, ~50-75 kJ mol^{-1}, is similar to those reported for granitoid weathering in other watersheds and laboratory experiments.